JPAC analyses of hadron spectroscopy

Alessandro Pilloni

NSTAR 2026, September 7th, 2026

Università degli Studi di Messina

EXOHAD
EXOTIC HADRONS TOPICAL COLLABORATION

INFN
CATANIA

The richness of hadron spectrum

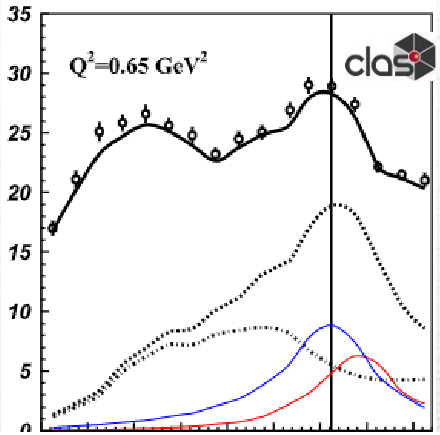

- The structures populating hadron reactions are extremely rich
- Ultimate goal is to understand them in term of QCD degrees of freedom
- To do so, the spectrum of resonances must be correctly reconstructed

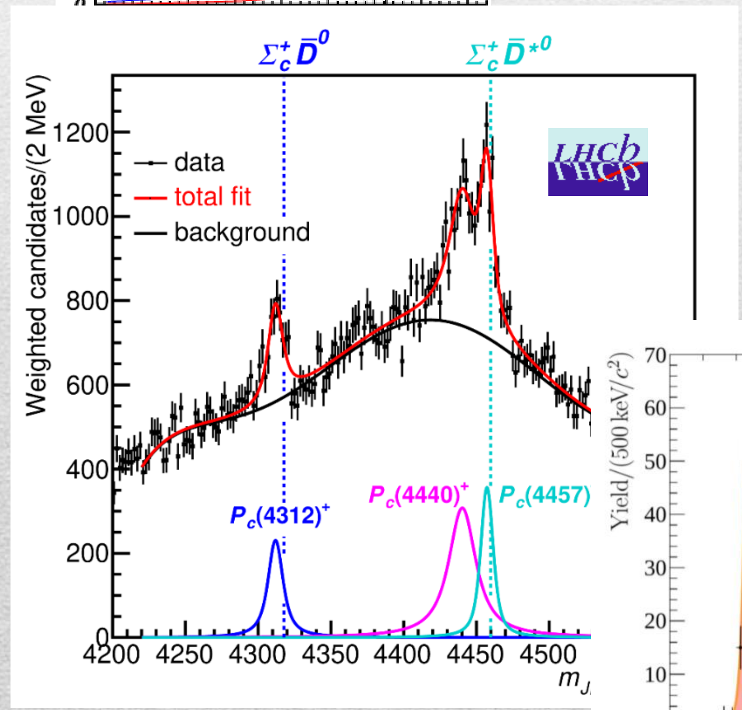

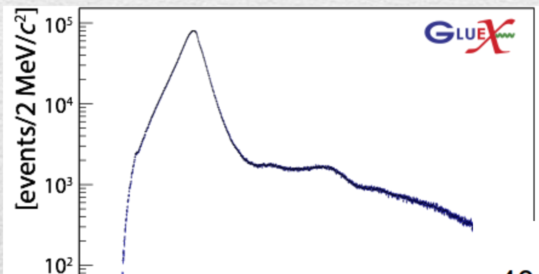

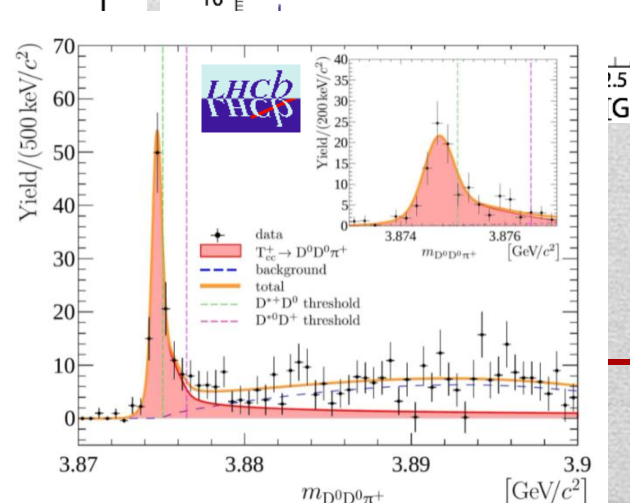

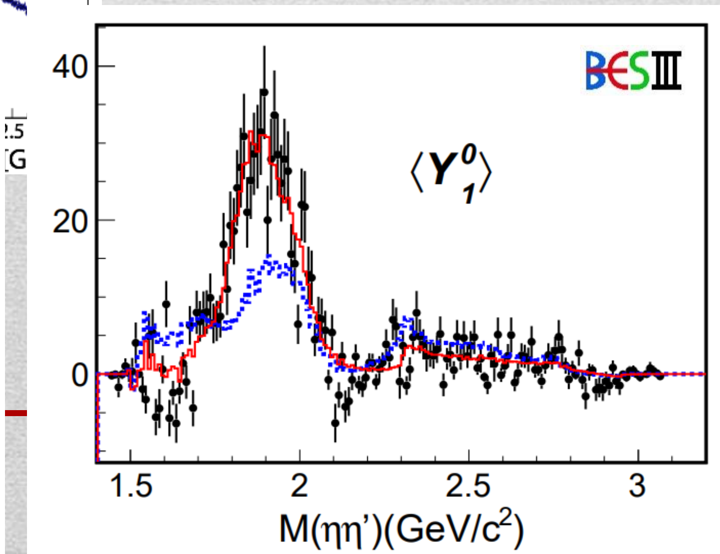

Bottom-up approach

Less predictive power ✘
Some physical interpretation ✘
Minimally biased ✓

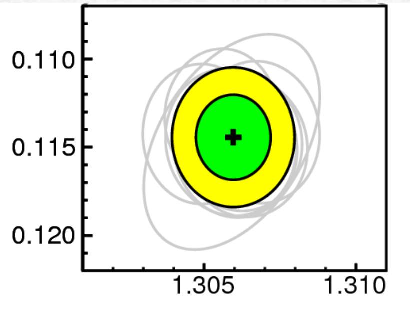

3) You extract physics

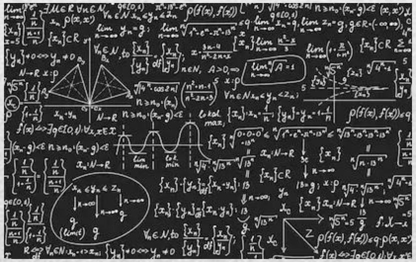

2) You choose a set of generic amplitudes

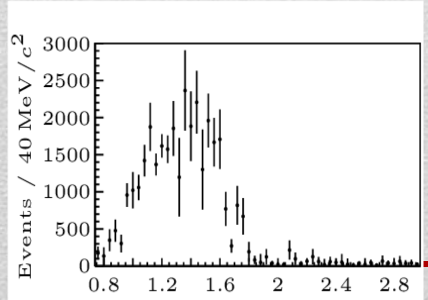

1) You start with data

S-Matrix principles

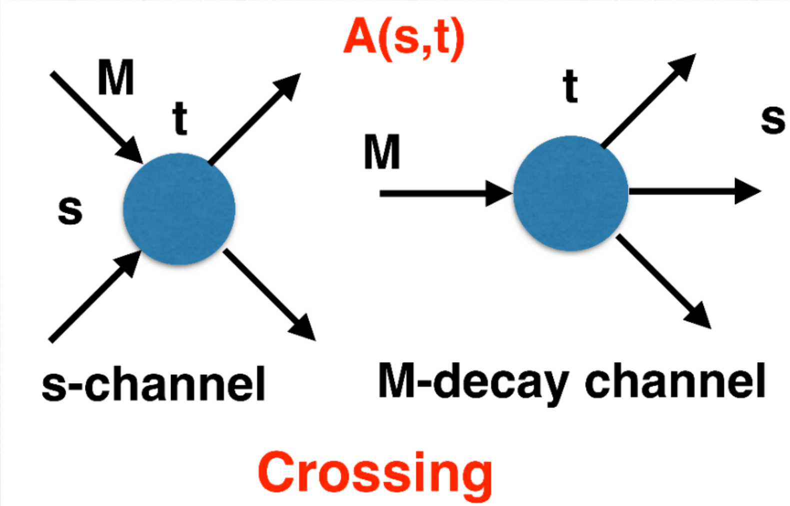

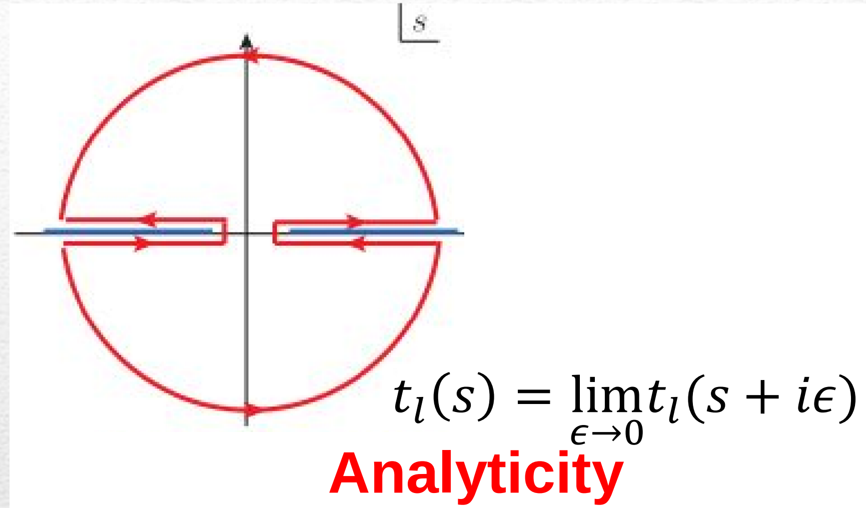

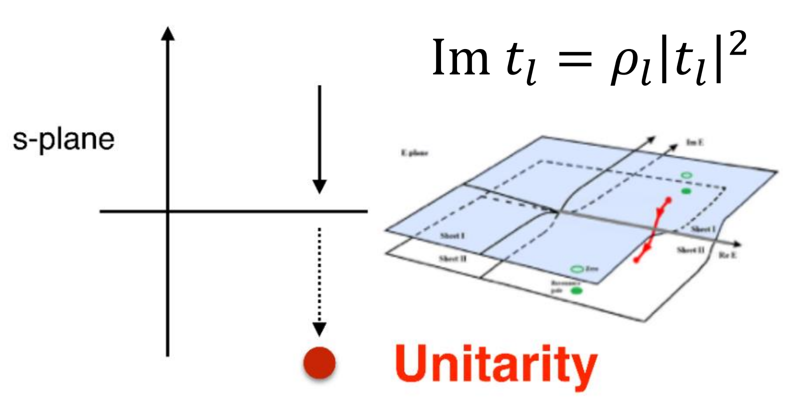

+ Lorentz, discrete & global symmetries

These are constraints the amplitudes have to satisfy, but do not fix the dynamics

They can be imposed with an increasing amount of rigor, to extract robust physics information

The «background» phenomena can be effectively parameterized in a controlled way

Joint Physics Analysis Center

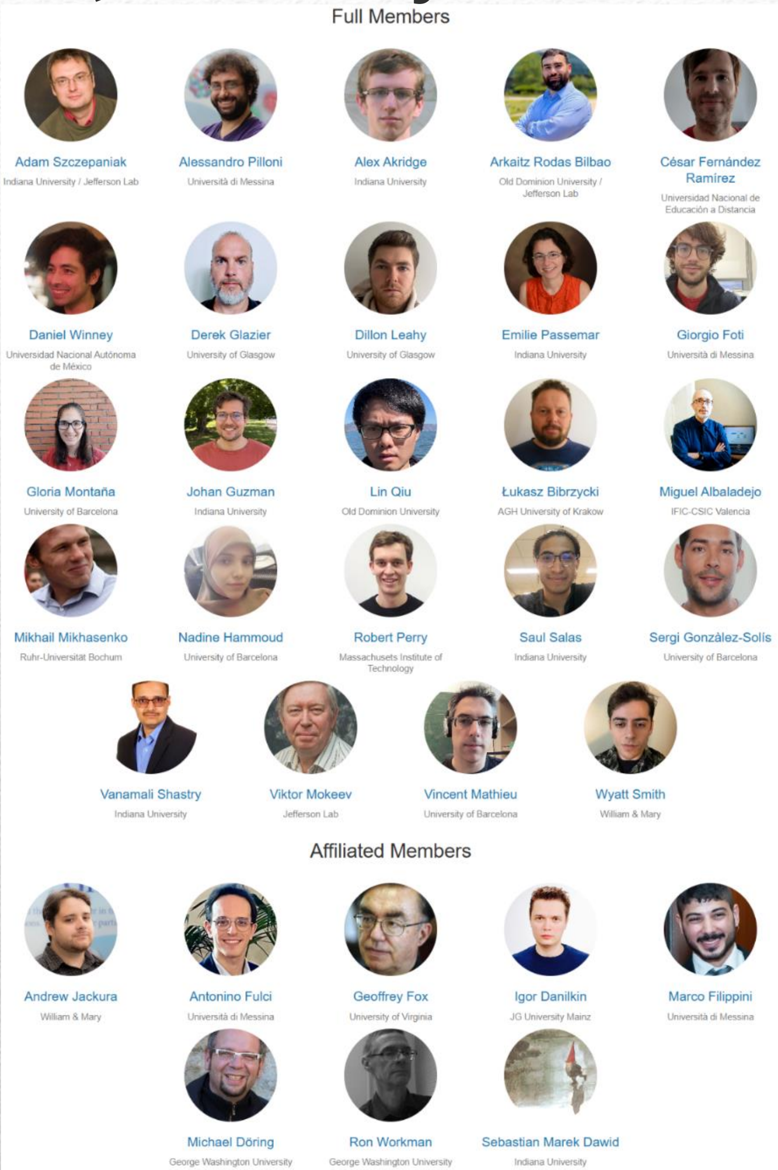

Funded in 2013 as theory support
originally for JLab exps, but grew up much larger

Creates bridges between
theorists and experimentalists

40+ researchers affiliated during a decade

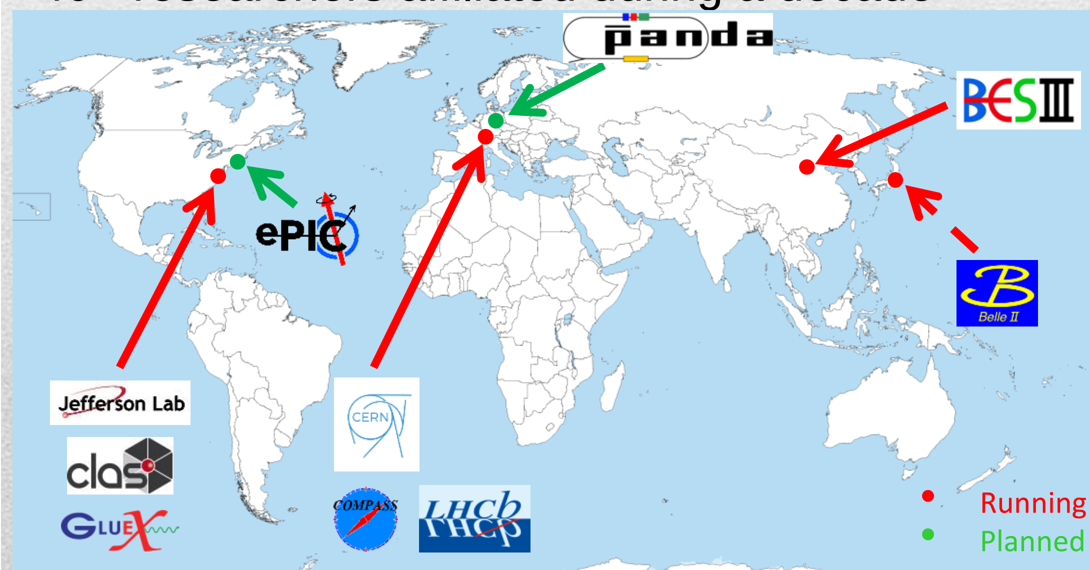

Exo(tic) Had(ron) TC

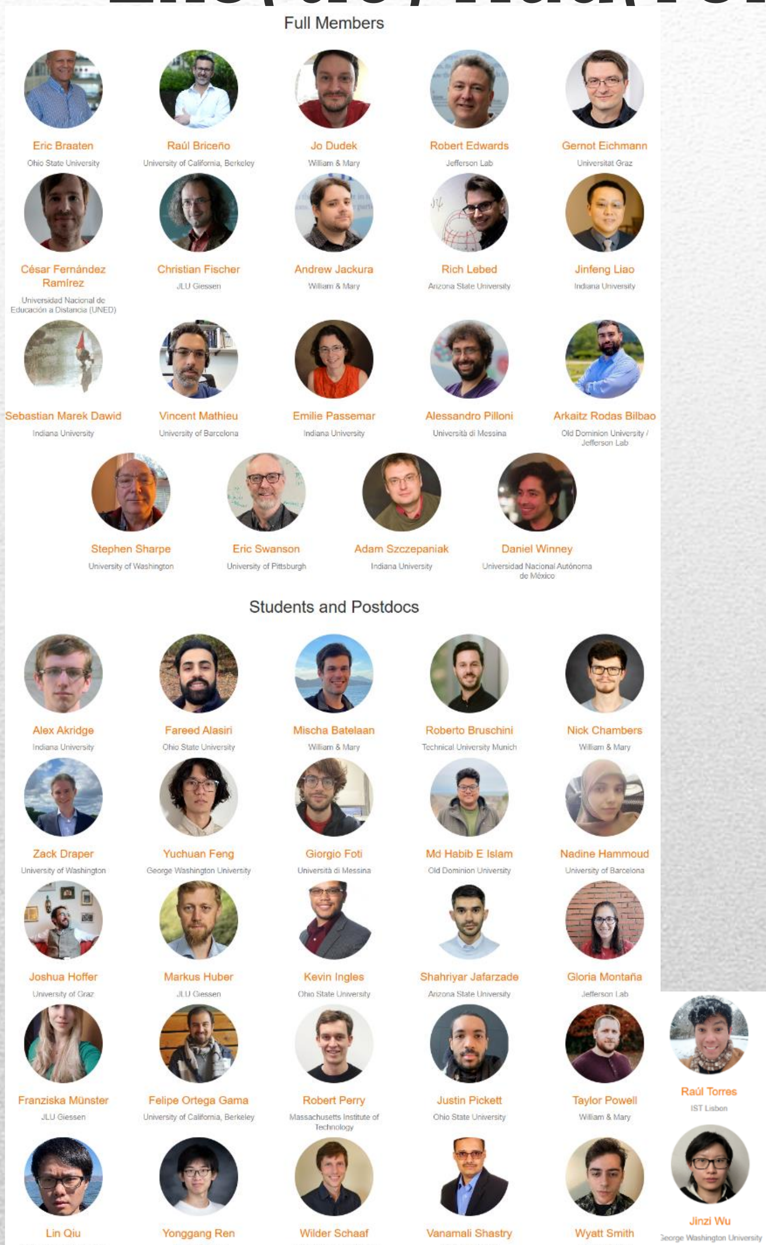

EXOHAD
EXOTIC HADRONS TOPICAL COLLABORATION

Funded in 2023 by DoE as a Topical Collaboration in Nuclear Physics

Aims at exploring all aspects of exotics (= hybrids at GlueX)

- Amplitude analysis
- Lattice QCD
- Phenomenology

copy

Semantic areas

Production mechanisms

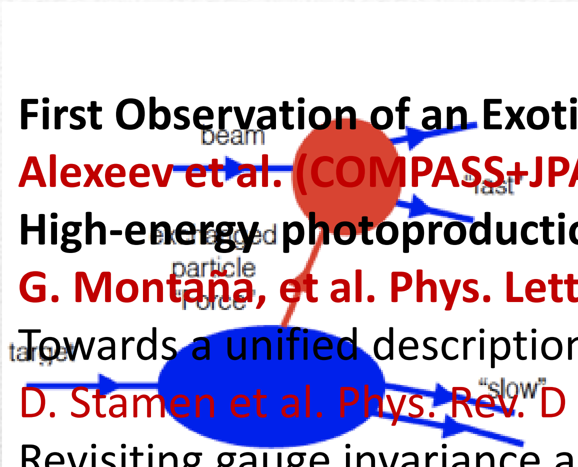

- **First Observation of an Exotic Reggeon**
  Alexeev et al. (COMPASS+JPAC), arXiv:2607.17850
- **High-energy photoproduction and the nature of exotic waves**
  G. Montaña, et al. Phys. Lett. B 872 (2026), 140101
- Towards a unified description of hadron scattering at all energies
  D. Stamen et al. Phys. Rev. D **110** (2024), 114023
- Revisiting gauge invariance and Reggeization of pion exchange
  G. Montaña et al. Phys. Rev. D **110** (2024), 114012
- Mechanisms of high energy polarized photoproduction of $\pi\Delta$
  V. Shastry, et al. arXiv:2604.22719, arXiv:2606.07917

→ See V. Mathieu's talk later

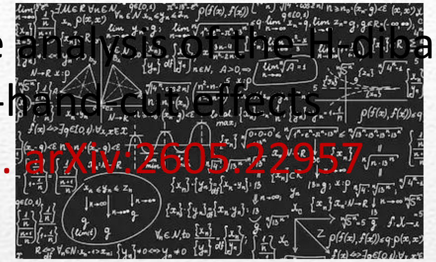

- Finite-volume analysis of the H-dibaryon including left-hand cut effects
  A. Rodas et al. arXiv:2605.22957

Formalism

Resonance physics

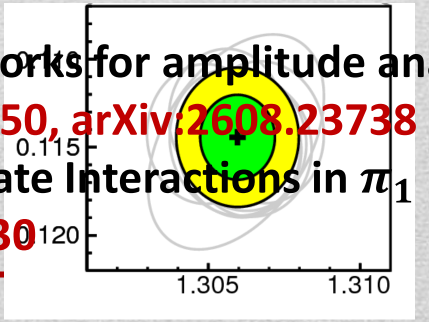

- **S-matrix informed neural networks for amplitude analysis**
  W. Smith *et al.*, arXiv:2608.23750, arXiv:2608.23738
- **Production Effects and Final-state Interactions in $\pi_1 \to 3\pi$**
  D. Winney et al. arXiv:2607.1430

S-Matrix informed Neural Networks

- $\pi\pi$ scattering is one of the most relevant processes
- It appears as final state for many production processes and hadronic decays
- I, J=0 is very interesting: Coupling to QCD vacuum, nonordinary resonances, glueball
- Directly tied to chiral symmetry-breaking phenomena

Problems

Light meson-scattering experiments are "modeled"

- Old experiments in the 70s and 80s
- Modern data only at very low energies

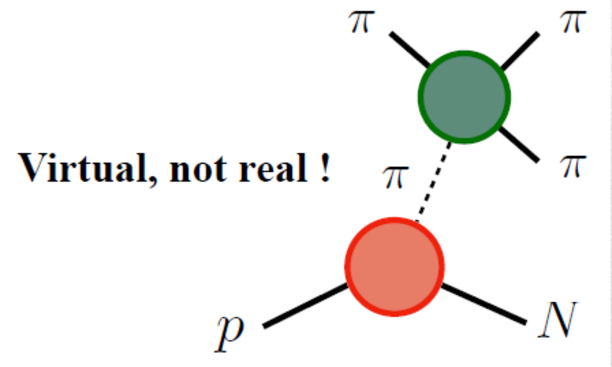

Modeling is unavoidable

- No known solutions to QCD
- Every model carries a bias (all are misspecified)
- The community has "given up" on addressing this issue

Fundamental principles are mandatory for accuracy

- Unitarity, analyticity, crossing symmetry constrain partial waves
- Analytic extrapolations are required to extract unstable particles

Systematics are propagated to other reactions

- FSI are fixed inputs to production
- Production analyses with common FSI are not analyzed together

S-Matrix informed Neural Networks

Smith *et al.*, arXiv:2608.23750, arXiv:2608.23738

Solution: SINN

Light meson-scattering experiments are "modeled"

- We will use NNs, together with data subset selection, to prune the database
- Quantitative, not perfect, but sensible and statistics based

Modeling is unavoidable

- NNs are incredibly flexible
- Parameter space is broad enough to cover large model space
- Uncertainties extracted from resamplings

Fundamental principles are mandatory for accuracy

- Impose unitarity by construction + analyticity and crossing through dispersion relations
- Use dispersion relations for robust analytic continuation

Systematics are propagated to other reactions

- If successful for FSI, can be extended to production
- Enough flexibility to describe "global" hadronic data

S-Matrix informed Neural Networks

Smith *et al.*, arXiv:2608.23750, arXiv:2608.23738

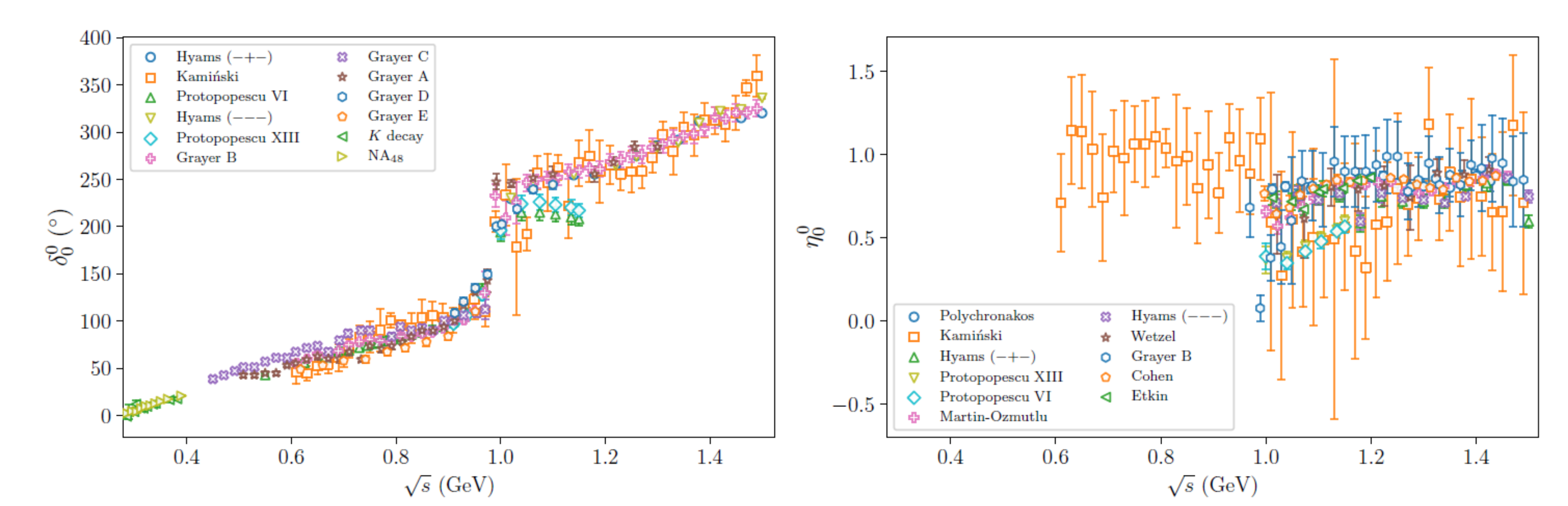

Data collected for 7 partial waves, over 1000 inconsistent initial data points, $\chi^2/DOF \sim 10$

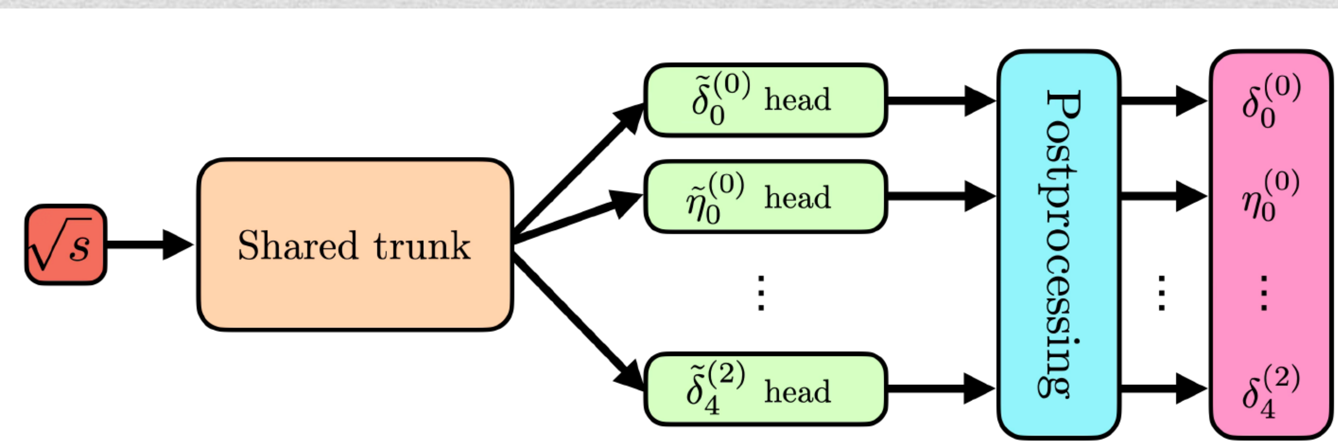

Hybrid multi-tasking architecture
Basic multi-output NNs needed 30 – 50 × more parameters

S-Matrix informed Neural Networks

Smith *et al.*, arXiv:2608.23750, arXiv:2608.23738

Unitarity will be given by construction

$$f_\ell^I(s) = \frac{\sqrt{s}}{2k}\frac{1}{2i}\left(\underbrace{\eta_\ell^I(s)}\, e^{2i\underbrace{\delta_\ell^I(s)}} - 1\right)$$

NN outputs

With $0 \leq \eta_\ell^I(s) \leq 1$

Crossing symmetry relates amplitudes in different channels and isospins

$$F^0(s,t) = \frac{1}{3}F^{(0)}(s,t) + F^{(1)}(s,t) + \frac{5}{3}F^{(2)}(s,t), \qquad F^1(s,t) = \frac{1}{3}F^{(0)}(s,t) + \frac{1}{2}F^{(1)}(s,t) - \frac{5}{6}F^{(2)}(s,t), \qquad F^2(s,t) = \frac{1}{3}F^{(0)}(s,t) - \frac{1}{2}F^{(1)}(s,t) + \frac{1}{6}F^{(2)}(s,t)$$

Mandelstam hyphotesis (all related to a singular analytic amplitude)

$$F^{I=0}(s,t,u) = 3\,F(s,t,u) + F(t,s,u) + F(u,t,s), \qquad F^{I=1}(s,t,u) = F(t,s,u) - F(u,t,s), \qquad F^{I=2}(s,t,u) = F(t,s,u) + F(u,t,s)$$

Dispersion relations offer a framework, by construction, to impose crossing symmetry

$$\underbrace{\mathrm{Re}\,\tilde{f}_\ell^I(s)} = \mathrm{ST}_\ell^I(s) + \mathrm{DT}_\ell^I(s) + \underbrace{\sum_{\ell' I'}} \mathrm{P.V.}\int_{4m_\pi^2}^{\infty} ds'\; K_{\ell,\ell'}^{I,I'}(s,s')\;\mathrm{Im}\; f_{\ell'}^{I'}(s')$$

The PW we want

All the relevant PWs contribute

S-Matrix informed Neural Networks

Smith *et al.*, arXiv:2608.23750, arXiv:2608.23738

First, losses are defined on a dynamic curriculum of weights (next slide), to speed up convergence and increase the success rate

Data is "fitted" with the following loss →

$$\mathcal{L}_{\text{data}} = \frac{1}{N_{\text{tot}}} \sum_{\alpha} \sum_{i=1}^{N_\alpha} \left[(1 - w_\chi)\, r_{\alpha,i}^2 + w_\chi \left(\frac{r_{\alpha,i}}{\sigma_{\alpha,i}} \right)^2 \right]$$

NN real output partial waves are forced to respect dispersive results

$$\text{Re}\, \tilde{f}_\ell^I(s) = \text{ST}_\ell^I(s) + \text{DT}_\ell^I(s) + \sum_{\ell' I'} \text{P.V.} \int_{4m_\pi^2}^{\infty} ds' \; K_{\ell,\ell'}^{I,I'}(s,s') \; \text{Im}\; f_{\ell'}^{I'}(s')$$

↓

$$\Delta_c(s) = \underbrace{\text{Re}\, \tilde{f}_c(s)}_{\textit{Dispersive}} - \underbrace{\text{Re}\, f_c(s)}_{\textit{NN}} \longrightarrow \mathcal{L}_{\text{Roy}} = \sum_{c \in \{S_0, P_1, S_2\}} \langle |\Delta_c(s)| \rangle_s$$

Scattering lengths are crucial fit and dispersive contributions

We create "free" SL parameters to constrain

Then use NN SLs as input in the last epochs

$$\longrightarrow \quad \mathcal{L}_{\text{SL}} = |a_0^0 - a_0^{0,\text{NN}}| + |a_0^2 - a_0^{2,\text{NN}}|$$

S-Matrix informed Neural Networks

Smith *et al.*, arXiv:2608.23750, arXiv:2608.23738

Curriculum of weights updated based on epoch (optimization steeps)

$$\mathcal{L}_{\text{total}} = \mathcal{L}_{\text{data}} + \lambda_{\text{Roy}}\mathcal{L}_{\text{Roy}} + \lambda_{\text{SL}}\mathcal{L}_{\text{SL}}$$

Epochs	λ_{data}	λ_{Roy}	λ_{SL}	w_χ
0–400	1	0	0	0.25
400–800	1	0.01	0.01	0.5
800–1000	1	0.5	0.1	0.75
1000–1200	1	1	1	1
1200–1500	1	1	10	1
1500–2000	1	2	Input	1

Example optimization

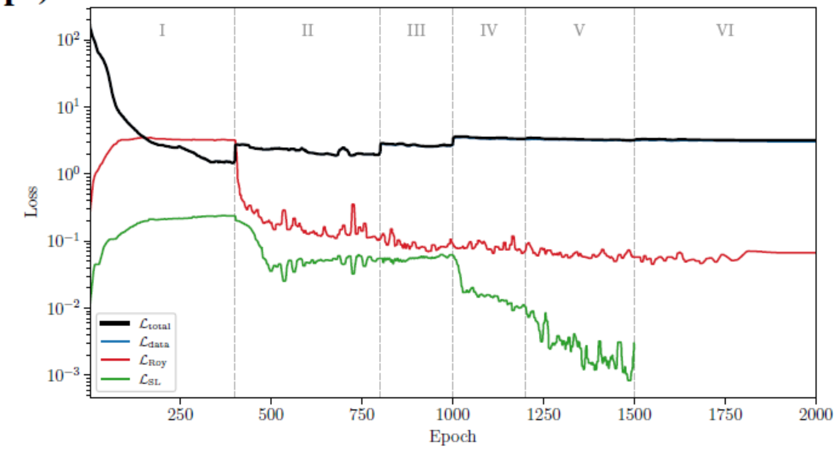

Propagation schema

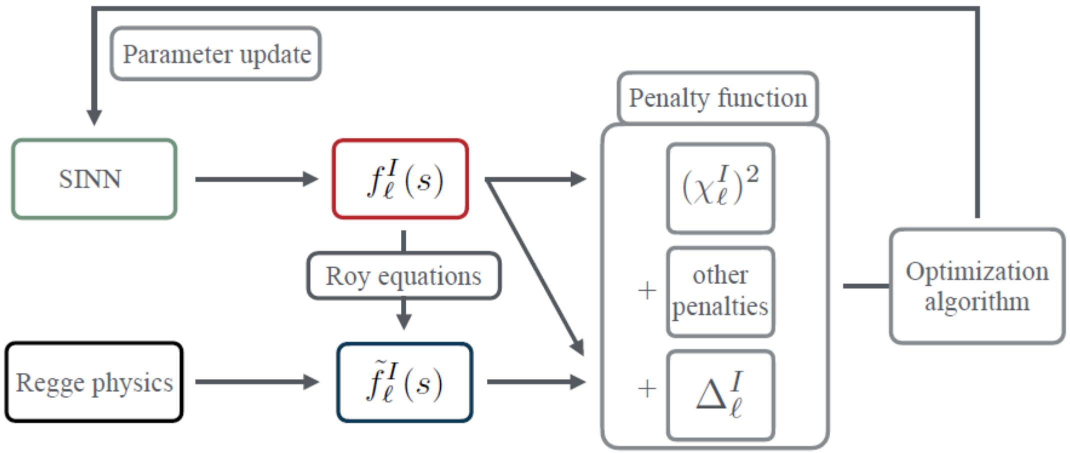

S-Matrix informed Neural Networks

Smith *et al.*, arXiv:2608.23750, arXiv:2608.23738

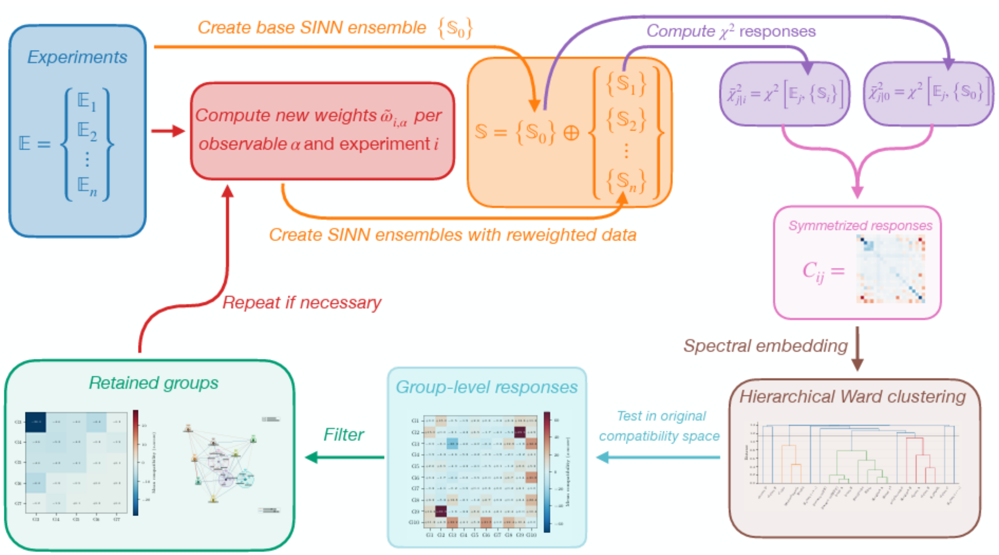

Observable	Included experiments
$\lvert a_0^0 - a_0^2\rvert$	DIRAC
S_0 phase	Grayer (A, B), Kamiński, K decay, NA48
S_0 inelasticity	Cohen, Etkin, Grayer B, Kamiński, Martin-Ozmutlu, Polychronakos, Wetzel
P_1 phase	Estabrooks, Hyams 73
P_1 inelasticity	Hyams 73
S_2 phase	Cohen, Durusoy (OPE, OPEDP), Hoogland (A,B), Losty (A,B)
S_2 inelasticity	Cohen, Losty B
D_0 phase	Hyams 73
D_0 inelasticity	Hyams 73
D_2 phase	Cohen, Durusoy (OPE, OPEDP), Hoogland (A,B), Losty (A,B)
F_1 phase	Hyams 73
F_1 inelasticity	Hyams 73
G_2 phase	Cohen, Durusoy (OPE, OPEDP), Losty B

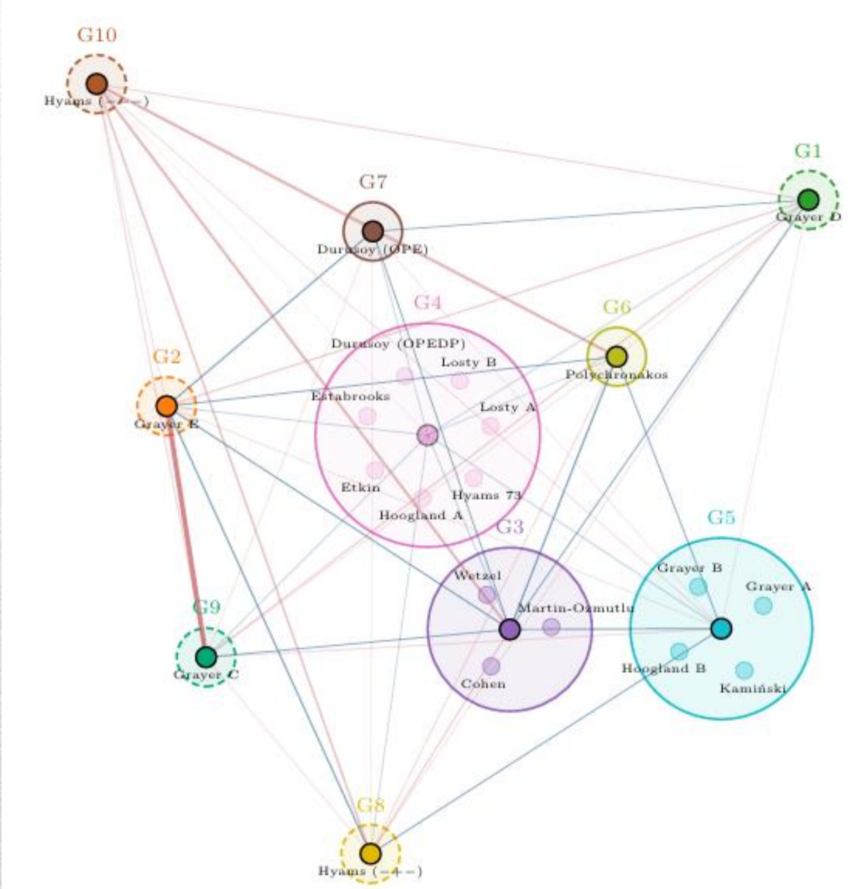

Results

Smith *et al.*, arXiv:2608.23750, arXiv:2608.23738

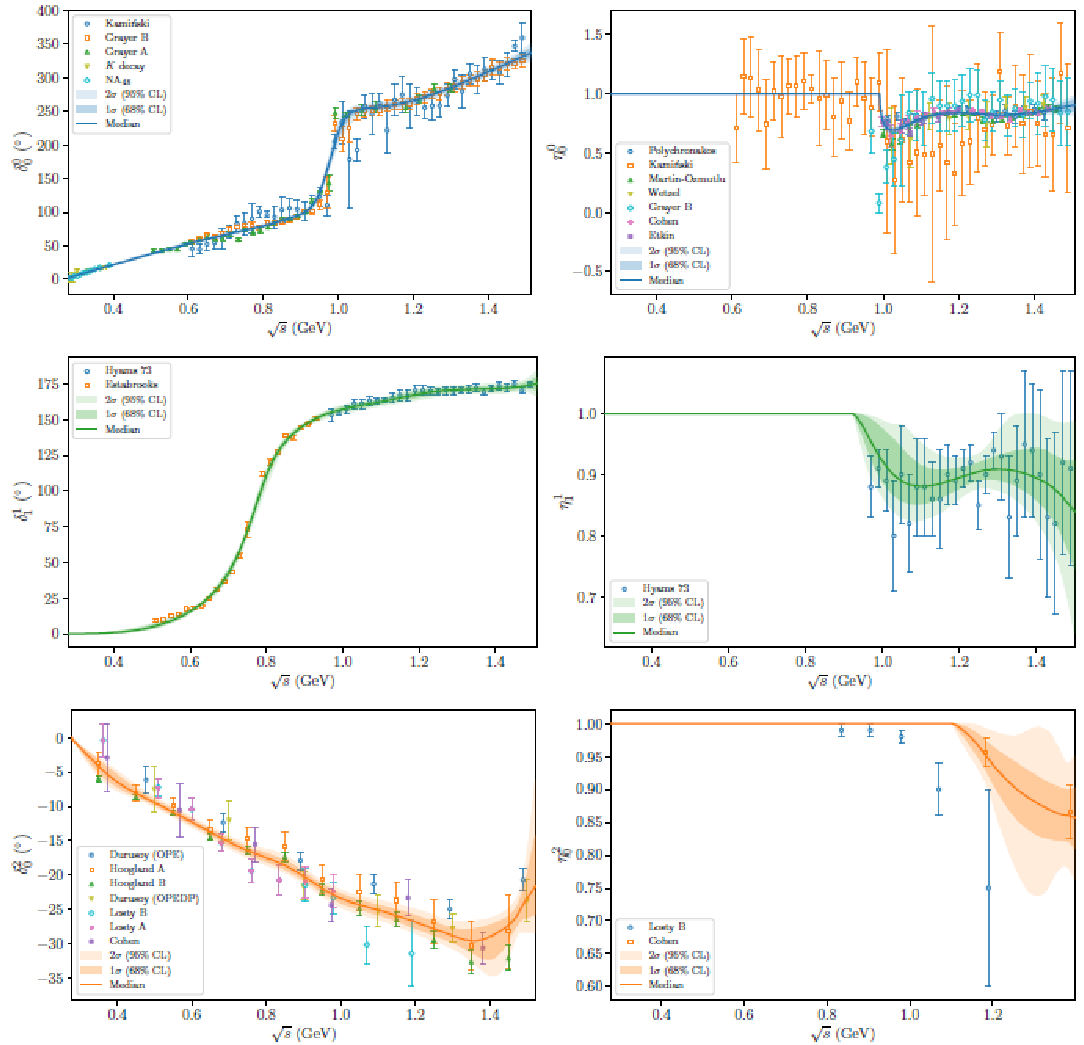

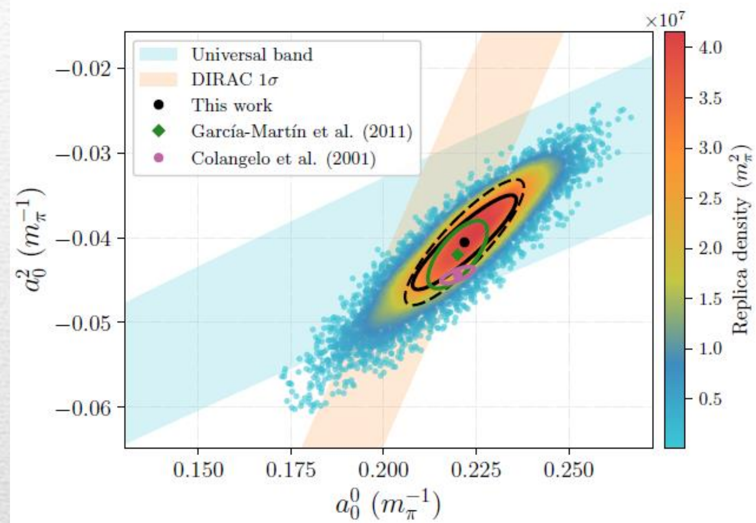

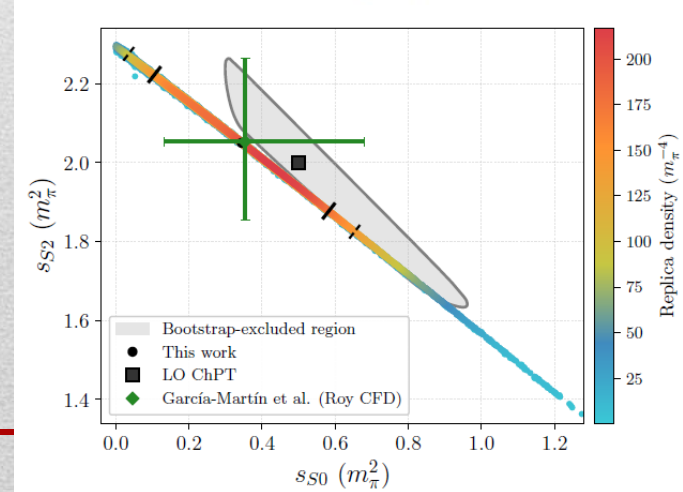

Results

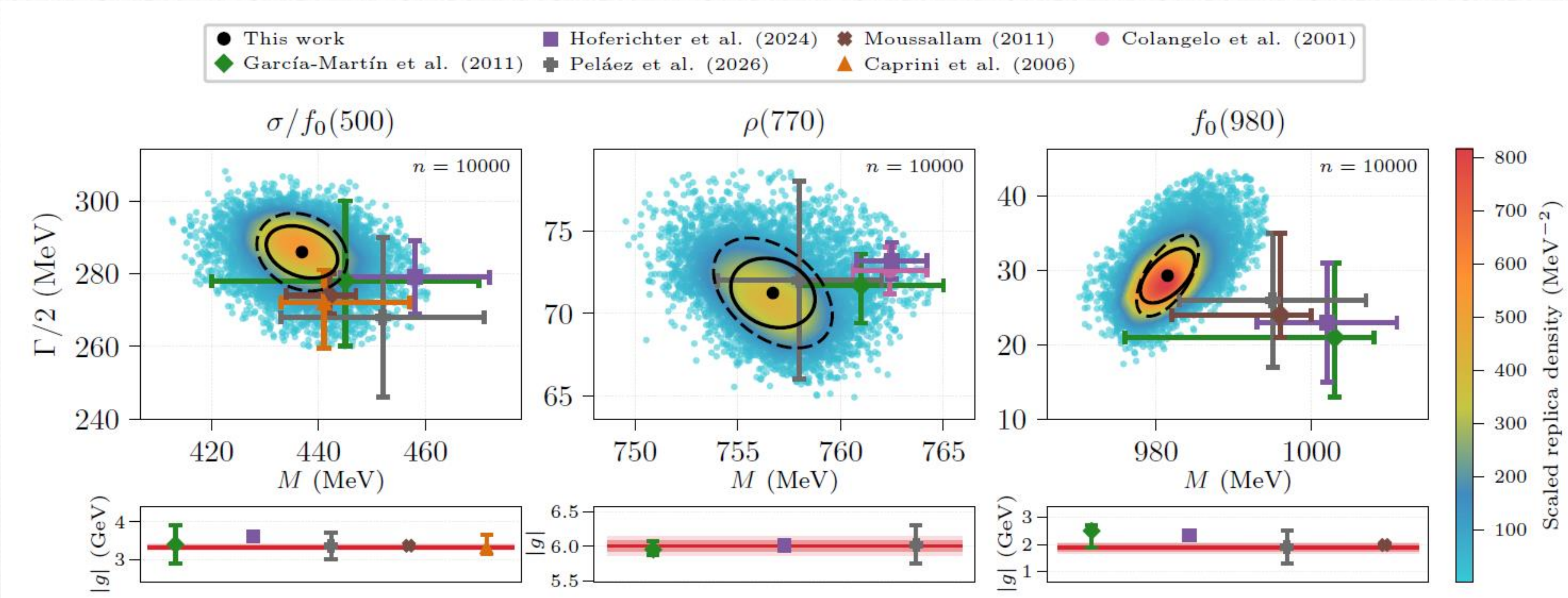

Reference	$\sqrt{s_{\sigma/f_0(500)}}$	$\lvert g_{\sigma\pi\pi}\rvert$	$\sqrt{s_{\rho(770)}}$	$\lvert g_{\rho\pi\pi}\rvert$	$\sqrt{s_{f_0(980)}}$	$\lvert g_{f_0\pi\pi}\rvert$
This work	$437^{+7}_{-6} - i\,286^{+6}_{-8}$	$3.33^{+0.06}_{-0.06}$	$757^{+2}_{-2} - i\,71^{+2}_{-2}$	$6.00^{+0.08}_{-0.07}$	$981^{+4}_{-3} - i\,29^{+4}_{-3}$	$1.87^{+0.15}_{-0.11}$
García-Martín et al. [32]	$445 \pm 25 - i\,278^{+22}_{-18}$	3.4 ± 0.5	$761^{+4}_{-3} - i\,71.7^{+1.9}_{-2.3}$	$5.95^{+0.12}_{-0.08}$	$1003^{+5}_{-27} - i\,21^{+10}_{-8}$	$2.5^{+0.2}_{-0.6}$
Colangelo et al. [57]	–	–	$762.4 \pm 1.8 - i\,72.6 \pm 1.4$	–	–	–
Hoferichter et al. [80]	$458 \pm 14 - i\,279 \pm 10$	3.61 ± 0.13	$762.5 \pm 1.7 - i\,73.2 \pm 1.1$	6.01 ± 0.08	$1002 \pm 9 - i\,23 \pm 8$	2.33 ± 0.18
Peláez et al. [33]	$452 \pm 19 - i\,268 \pm 22$	3.36 ± 0.36	$758 \pm 4 - i\,72 \pm 6$	6.025 ± 0.275	$995 \pm 12 - i\,26 \pm 9$	1.9 ± 0.6
Moussallam [81]	$442^{+5}_{-8} - i\,274^{+6}_{-5}$	3.37	–	–	$996^{+4}_{-14} - i\,24^{+11}_{-3}$	1.98
Caprini et al. [39]	$441^{+16}_{-8} - i\,272^{+9}_{-13}$	$3.31^{+0.35}_{-0.15}$	–	–	–	–
Guerrieri et al. [67]	$413 \pm 3 - i\,289 \pm 3$	–	$765.6 \pm 0.7 - i\,74.3 \pm 0.3$	–	$991 \pm 6 - i\,36 \pm 3$	–

$\pi_1 \to 3\pi$ with freed-isobars at COMPASS

Winney et al. arXiv:2607.1430

Using the huge 3π COMPASS data set, extract **line-shape of $\pi\pi$ subsystems** in the $\rho\pi$ P-wave

152 Dalitz plots as a function of t and $m_{3\pi}$

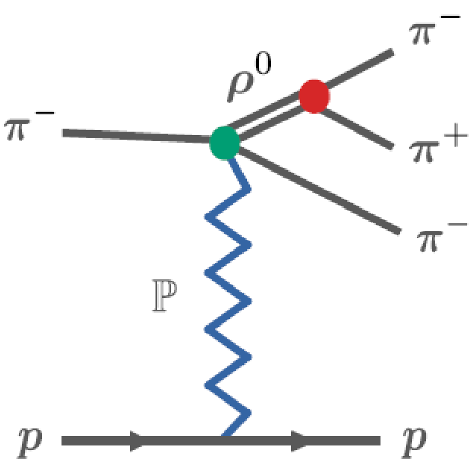

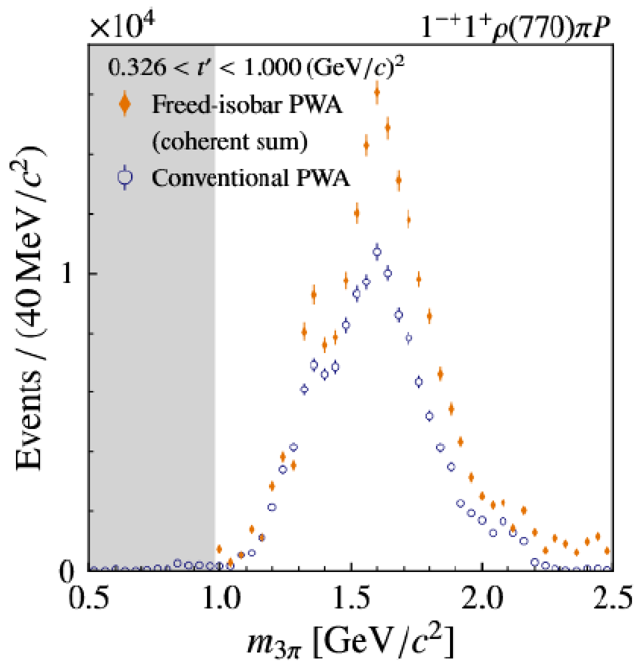

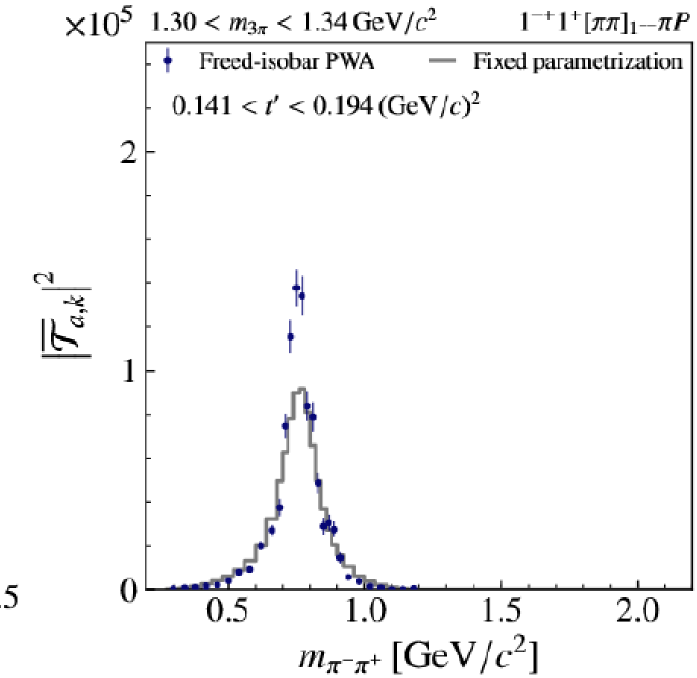

COMPASS [Phys.Rev.D 105 (2022) 1, 012005]

$\pi_1 \to 3\pi$ and Deck

Winney et al. arXiv:2607.1430

Production via intermediate particle exchange can generate **logarithmic singularities** which can mimic resonances

Deck [Phys.Rev.Lett. 13 (1964) 169-173]

$$\frac{1}{2}\int \frac{d\cos\theta}{\mu^2 - \tau(\cos\theta)} = \frac{1}{2qk}\log\left(\frac{\zeta+1}{\zeta-1}\right) = \frac{1}{qk}Q_0(\zeta)$$

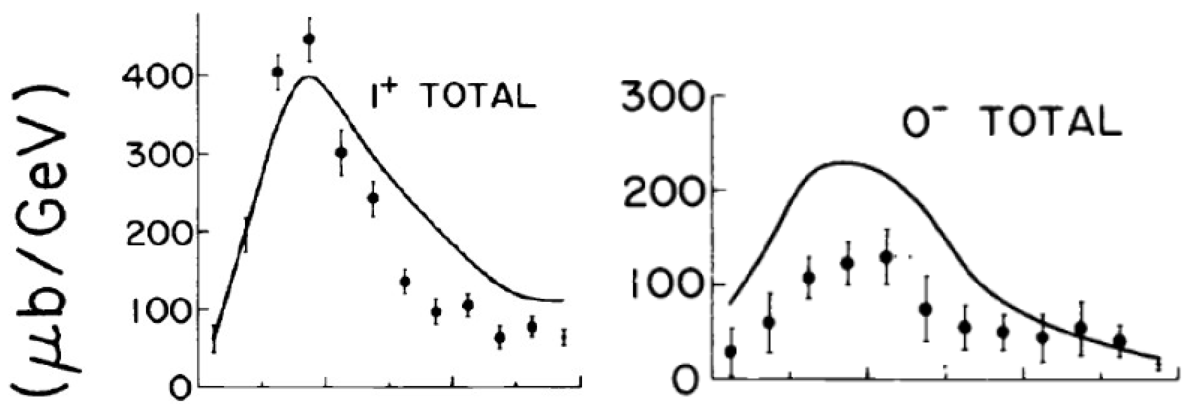

Ascoli et al. [Phys.Rev.D9(1974)1963-1979]

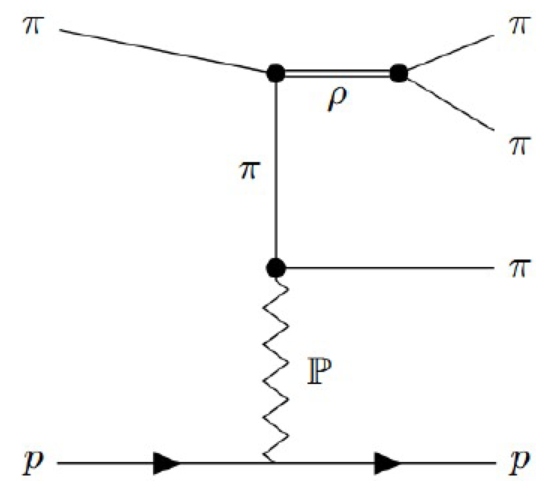

Khuri-Treiman

Winney et al. arXiv:2607.1430

Imposing **two-body unitarity** yields system of coupled, inhomogeneous integral equations which need to be solved numerically

$$F(\sigma) = B(\sigma) + \frac{\sigma^n}{\pi} \int \frac{d\sigma'}{(\sigma')^n} \frac{\text{Disc } F(\sigma')}{\sigma' - \sigma}$$

$$\text{Disc } F(\sigma) = \sin\delta(\sigma)\, e^{i\delta(\sigma)} \left[F(\sigma) + \int d\sigma'\, K(\sigma,\sigma')\, F(\sigma') \right]$$

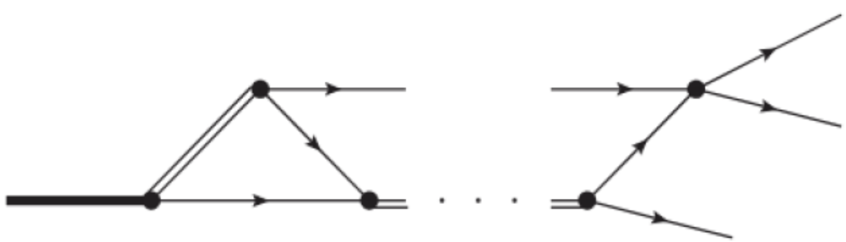

$$F(\sigma) = B(\sigma) + \frac{\sigma^n}{\pi} \int \frac{d\sigma'}{(\sigma')^n} \frac{\text{Disc } F(\sigma')}{\sigma' - \sigma}$$

The **Born term** parameterizes any effects not constrained by unitarity (i.e. production left-hand cuts!)

$$B_{\text{Deck}}(t, m_{3\pi}^2; \sigma) = N_d(m_{3\pi}^2)\, \sqrt{t}\, e^{dt}\, \Delta(t, m_{3\pi}^2; \sigma)$$

$$\Delta(t, m_{3\pi}^2; \sigma) = \frac{\rho_{\pi\rho P}}{qk} \left[(1-\zeta^2)\, Q_0(\zeta) + \zeta \right]$$

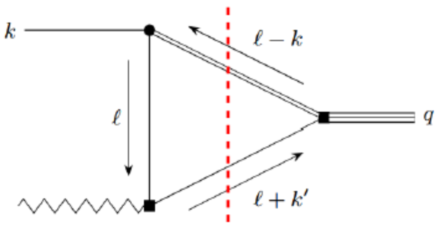

Deck mechanism

Khuri-Treiman

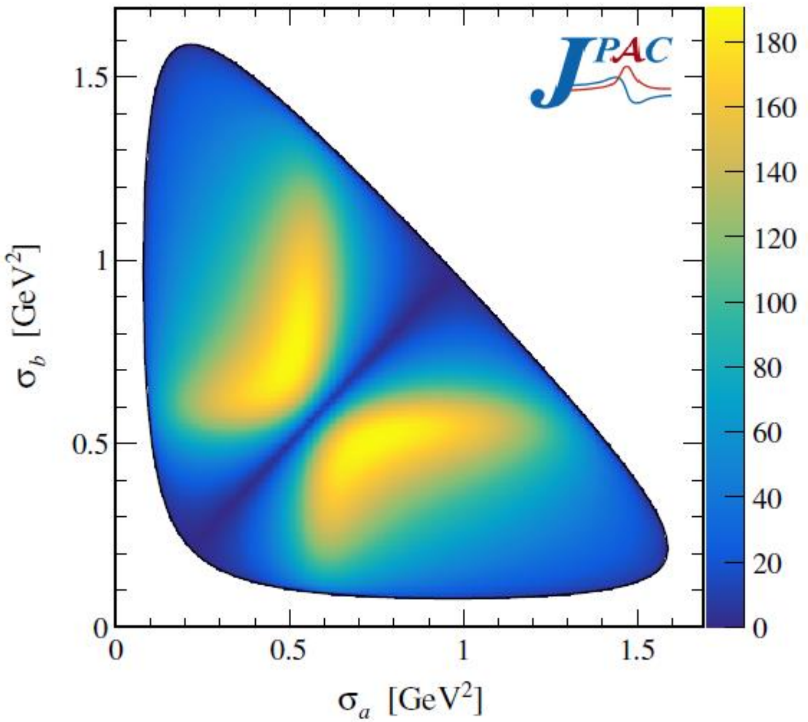

FIG. 8. Dalitz plot intensity using the CD isobar at $m_{3\pi} = 1.4$ GeV and $t = t_0 = -0.12$ GeV^2.

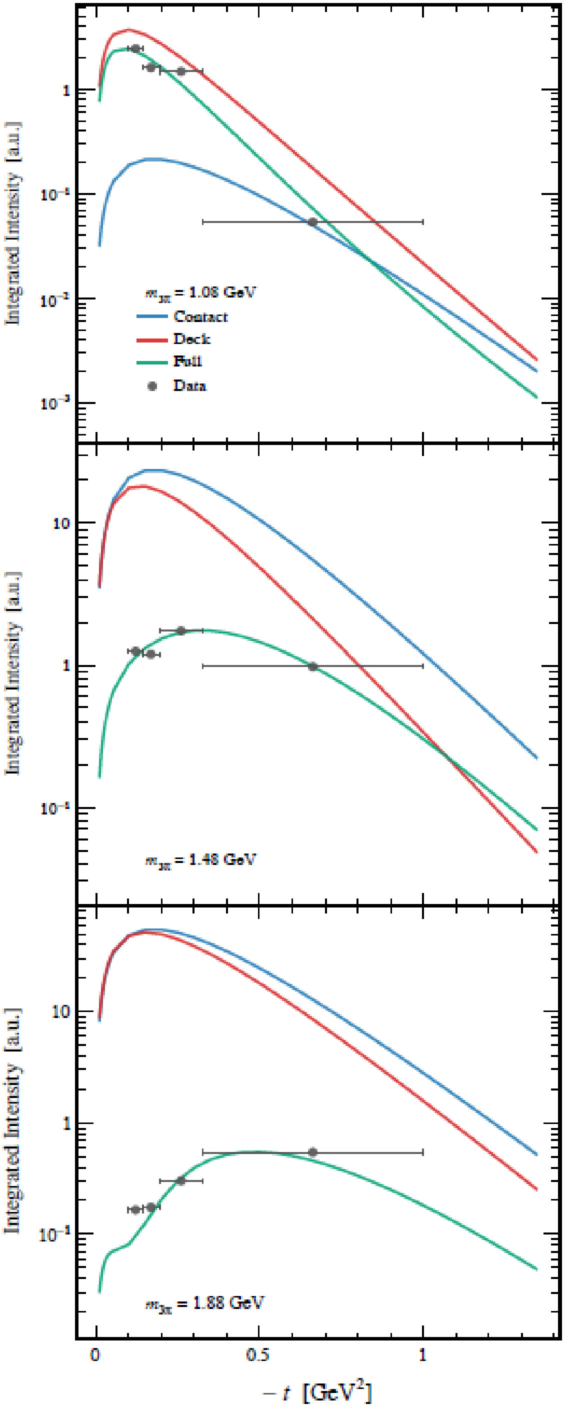

Khuri-Treiman

Winney et al. arXiv:2607.1430

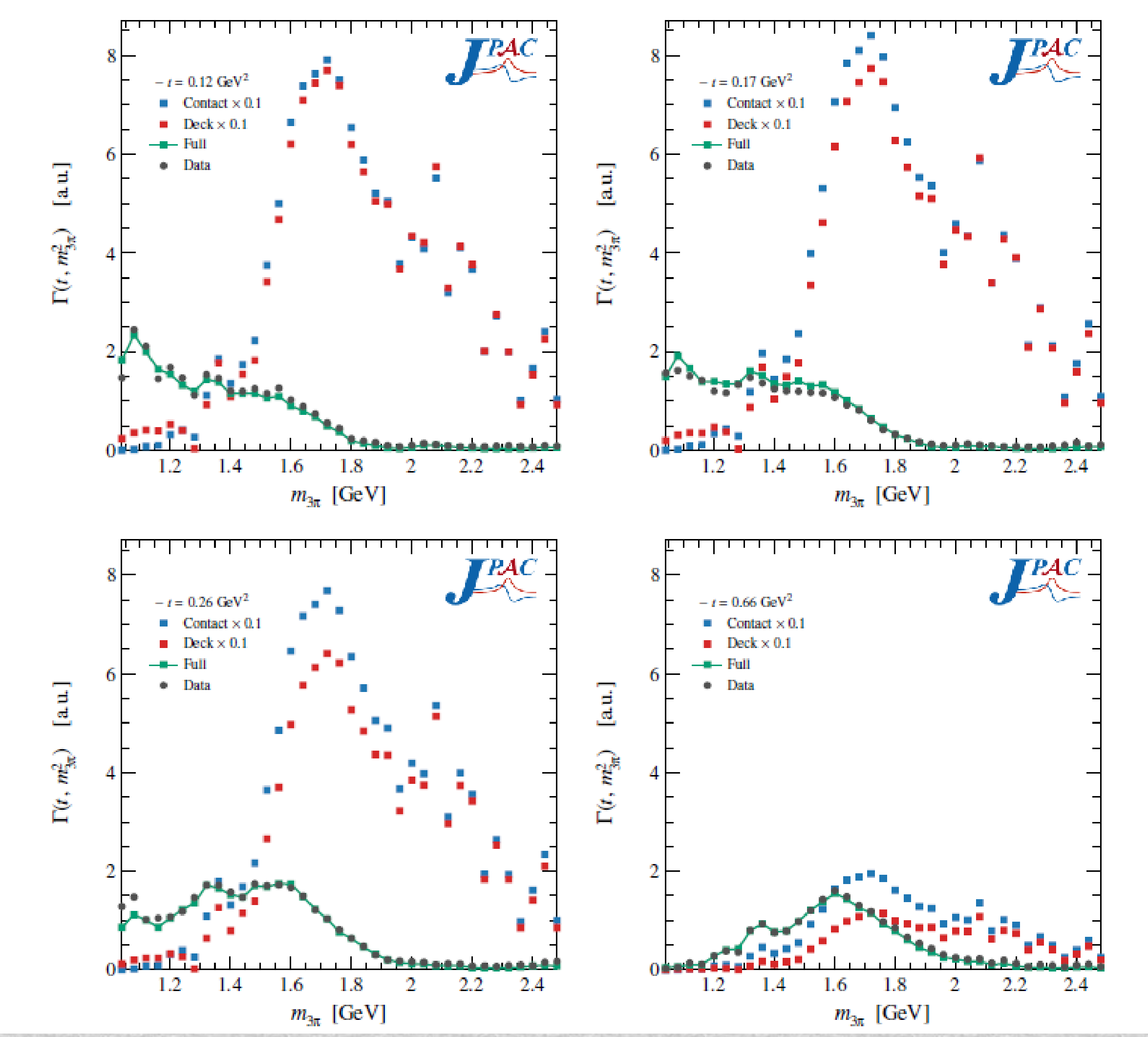

Spectroscopy from peripheral production

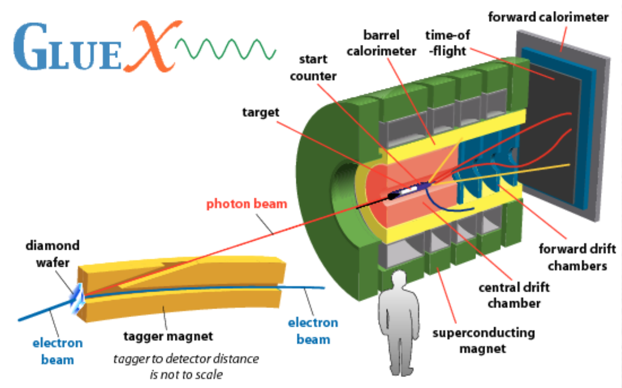

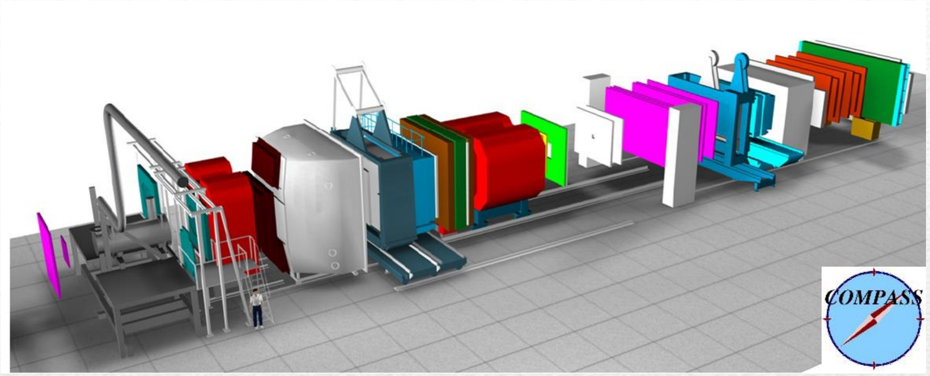

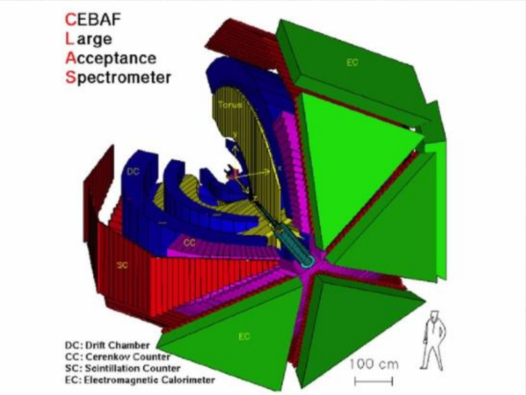

Need to establish Regge factorization

Single Regge pole dominate

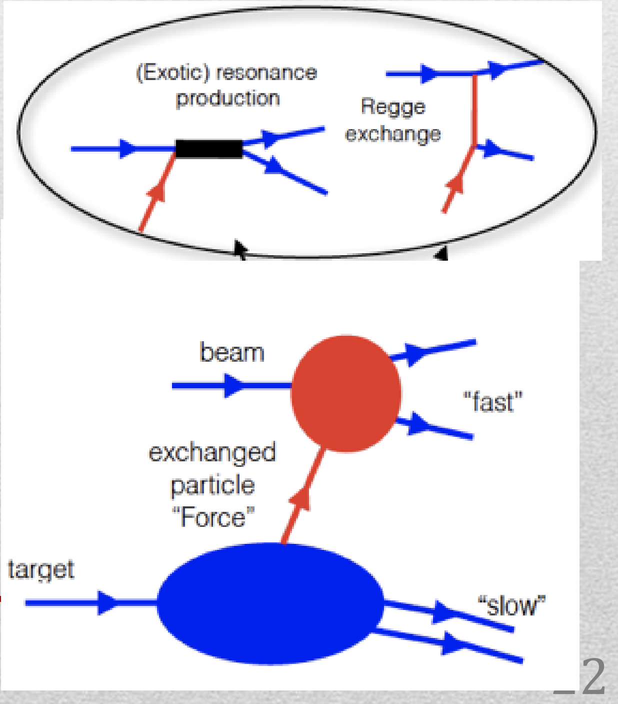

A Regge theory primer

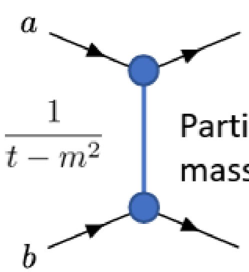

Particle with mass m and spin J

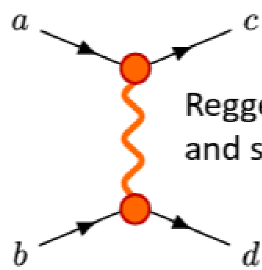

Reggeon with mass $\sqrt{t}$ and spin $\alpha(t)$

$$\mathcal{P}_{\text{Regge}} = \underbrace{\frac{\pi\alpha'}{\sin\left(\pi\alpha(t)\right)}}_{\text{poles for integer } \alpha(t)} \underbrace{\frac{1+\eta e^{-i\pi\alpha(t)}}{2}}_{\text{signature factor } \xi(t)} \underbrace{\left(\frac{s}{s_0}\right)^{\alpha(t)}}_{\text{asymptotic behavior}} \underbrace{\frac{1}{\Gamma\left(1+\alpha(t)\right)}}_{\text{cancel non-physical poles}}$$

V.Mathieu et al., *Phys.Rev.D* 98, 014041 (2018)

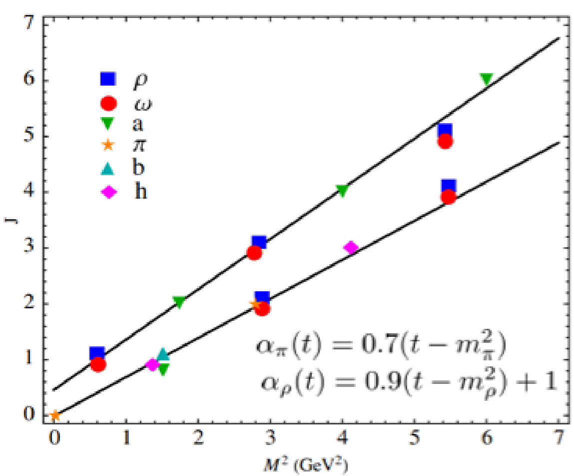

Resonances appear simultaneously as poles in energy and spin!

- **Regge trajectories:** families with same quantum numbers but different spin
- Almost straight lines (Chew-Frautschi plot)
- In standard Regge theory parameterized by $\alpha(t) = \alpha' t + \alpha_0$

G. Montaña

Single Regge and double Regge

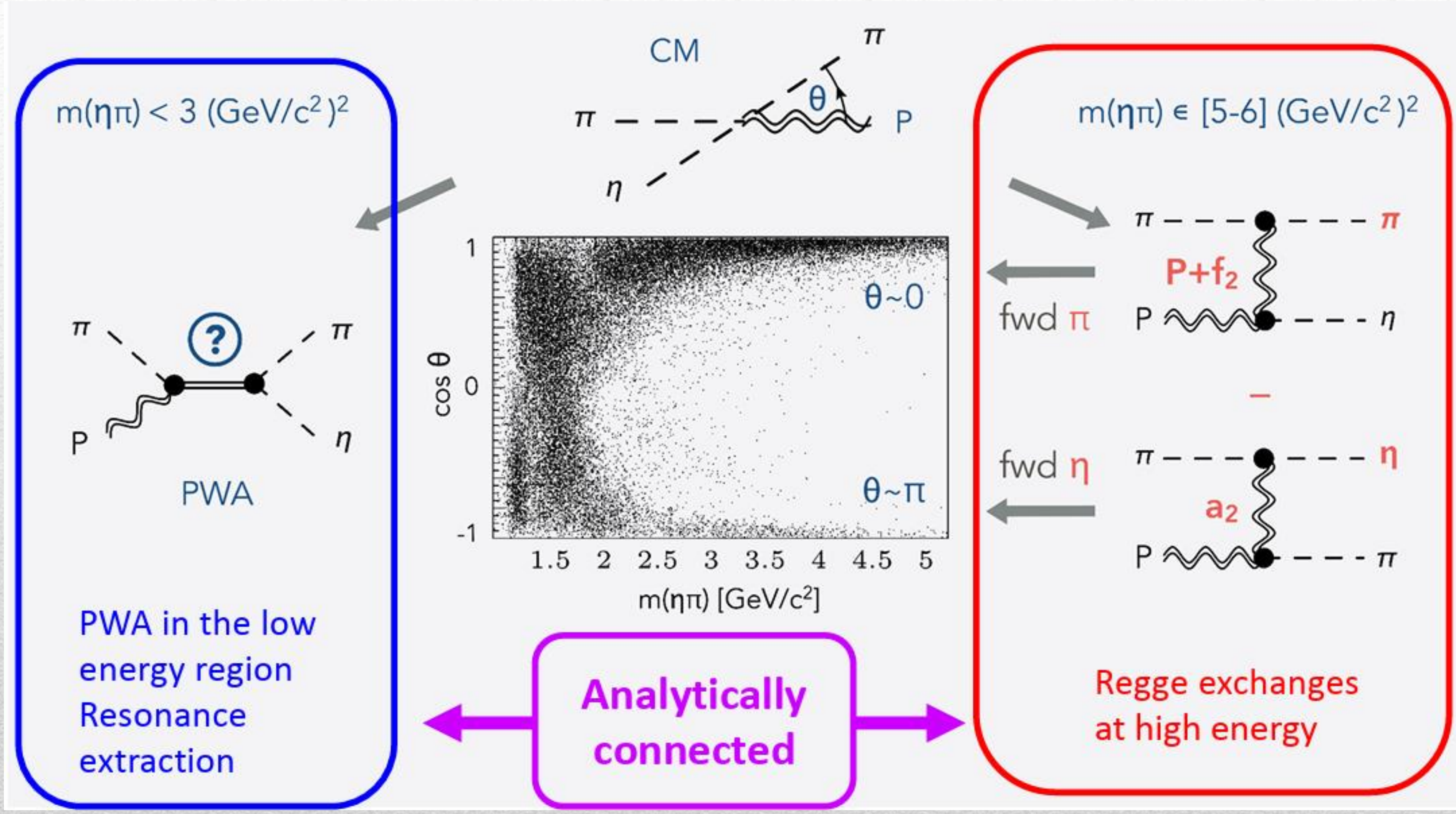

$\eta^{(\prime)}\pi$ photoproduction in the double Regge region

Montana *et al.*, PLB**872**, 140101

- Double Regge model based on double vector-meson exchanges with no free parameters
- Comparison to CLAS data (not a fit):

[Phys. Rev. C 102, 032201 (2020)]

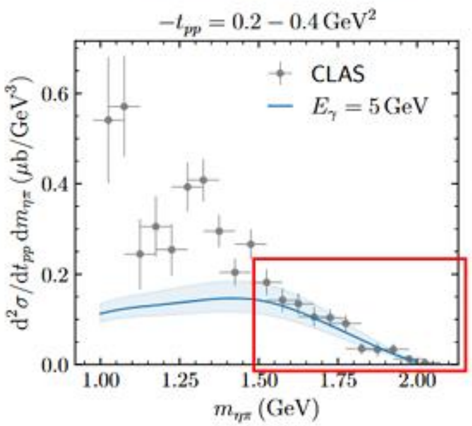

Shaded band:

$0.95\ \mathrm{GeV}^2 < s_0 < 1.05\ \mathrm{GeV}^2$

- Predictions for GlueX energy

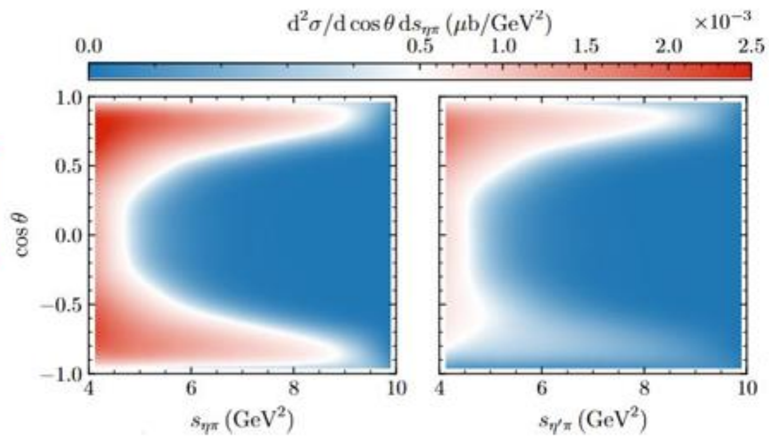

- **Forward-backward asymmetry implies odd (exotic) waves**

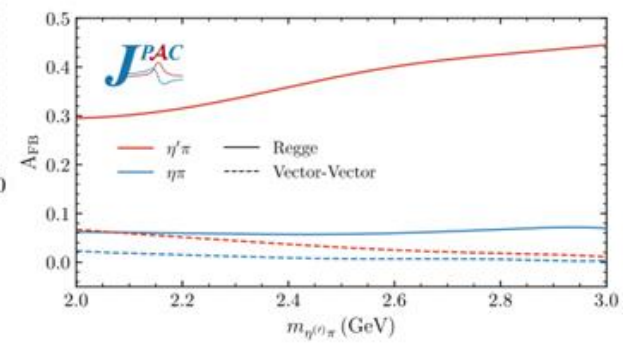

Large asymmetries not necessarily motivated by Pomeron (gluonic) exchanges

$\eta^{(\prime)}\pi$ at COMPASS

COMPASS+JPAC, arXiv:2607.17850

COMPASS has high-statistics $\eta^{(\prime)}\pi$ samples extending to $m_{\eta\pi} = 6$ GeV
Above about 2 GeV, events concentrate in forward/backward regions
These regions correspond to one produced meson carrying most of the beam momentum
This is where double-Regge exchange is expected to dominate

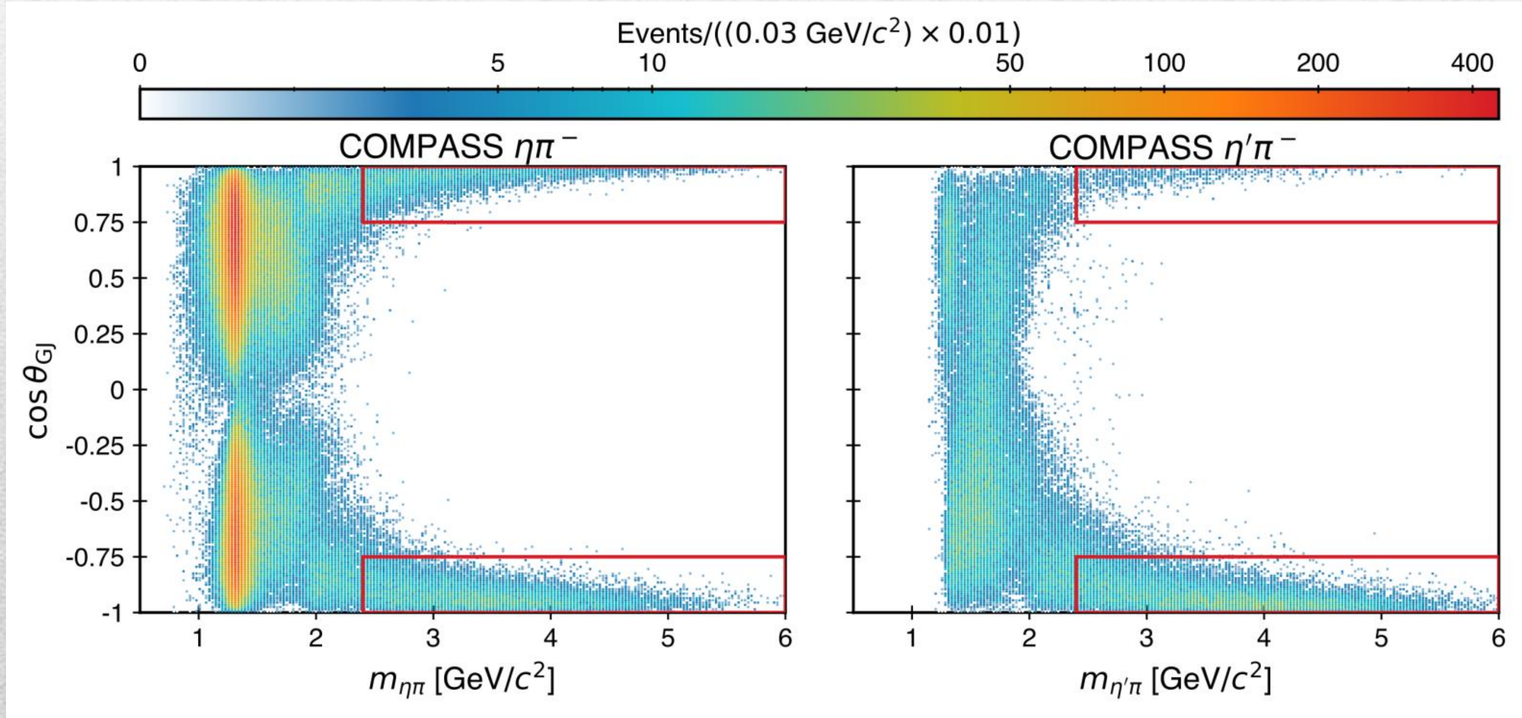

$\eta^{(\prime)}\pi$ at COMPASS

COMPASS+JPAC, arXiv:2607.17850

Backward / fast π
- top exchange connects: $\pi^- \to \pi^-$
- leading exchanges: $\mathbb{R}_t = \mathbb{P}, f_2$
- Odd spin exchanges are forbidden by Bose symmetry

Forward / fast $\eta^{(\prime)}$
- top exchange connects: $\pi^- \to \eta^{(\prime)}$
- allowed natural-parity isovector exchanges: $\mathbb{R}_t = a_2, a_2', \pi_1$ where
  - a_2: leading ordinary positive-signature
  - a_2': subleading ordinary positive signature exchange
  - π_1: exotic negative-signature

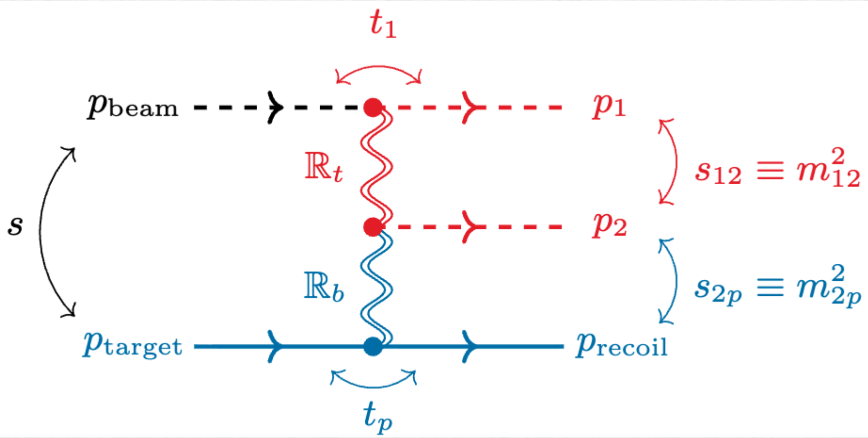

Signature $\xi = (-)^J$ controls the momentum transfer dependence

$\eta^{(\prime)}\pi$ at COMPASS

COMPASS+JPAC, arXiv:2607.17850

- Event-by-event extended negative log-likelihood fit (24k $\eta\pi^-$ events and 21k $\eta'\pi^-$ events)
- Acceptance handled using COMPASS Monte Carlo propagated through **TGEANT**
- Parameters include real amplitude strengths and exponential t-slope form factors
- Variations in the Regge trajectories are considered
- Fits performed independently for $\eta\pi^-$ and $\eta'\pi^-$
- The unbinned analysis preserves angular and momentum-transfer correlations that would be washed out in a simpler binned projection

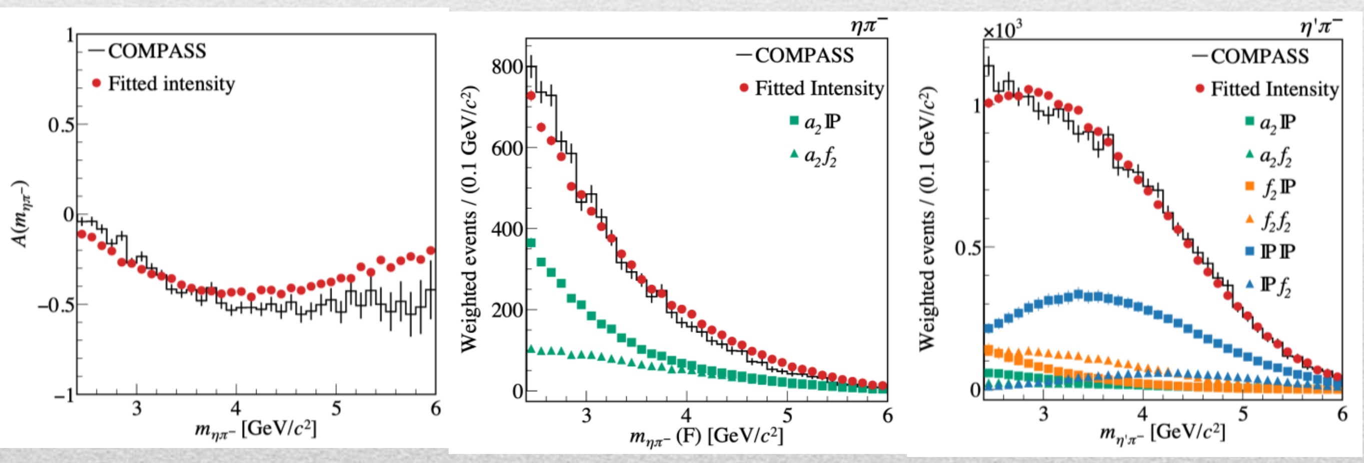

The base model does not describe the distributions in the forward peak

Missing physics in the top exchange

An exotic Reggeon is required

Hypotheses compared		H_1 significance	
H_0	H_1	$\eta\pi^-$	$\eta'\pi^-$
Base	Base+a_2'	11.0σ	10.1σ
Base	Base+π_1	12.8σ	11.7σ
Base	Base+$a_2' + \pi_1$	15.4σ	12.2σ
Base+a_2'	Base+$a_2' + \pi_1$	9.9σ	5.5σ
Base+π_1	Base+$a_2' + \pi_1$	2.2σ	disfavored

Something else is needed

That something is an exotic Reggeon

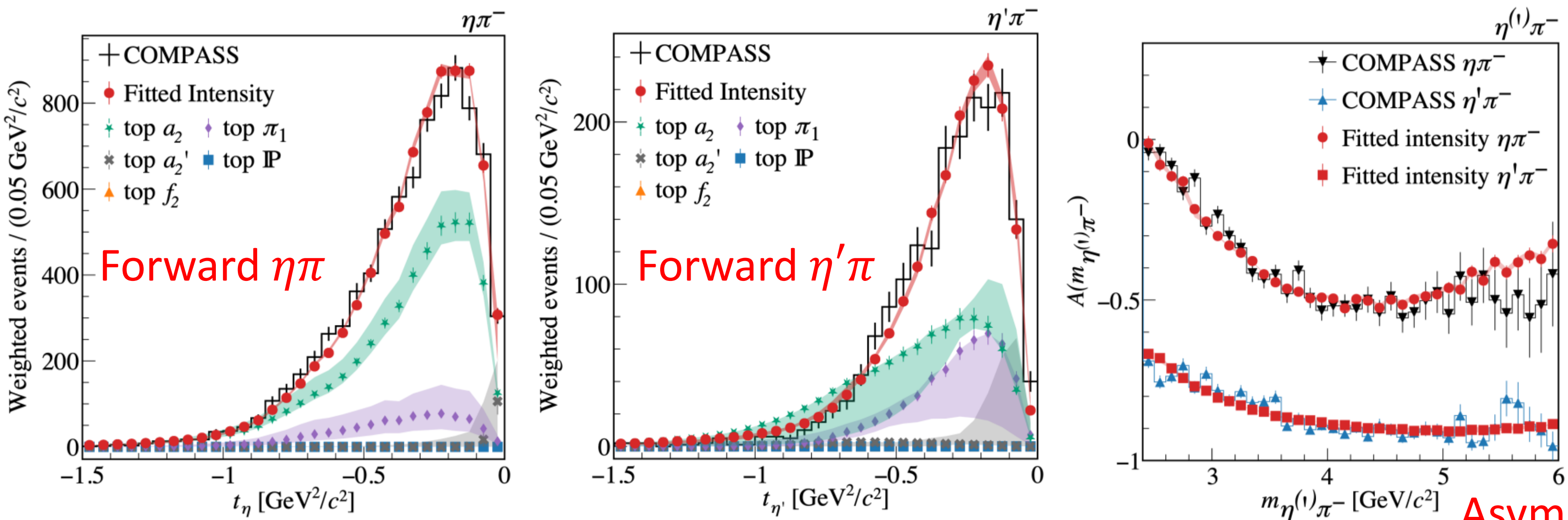

Asymmetry

Backward peak

COMPASS+JPAC, arXiv:2607.17850

- High statistics allow to disentangle the bottom vertex
- Bottom Pomeron dominates in both $\eta\pi^-$ and $\eta'\pi^-$ channels
- However, bottom f_2 exchange is not negligible, especially at the smallest proton momentum transfer
- This matters for future diffractive analyses: assuming pure Pomeron exchange may be insufficient at COMPASS kinematics

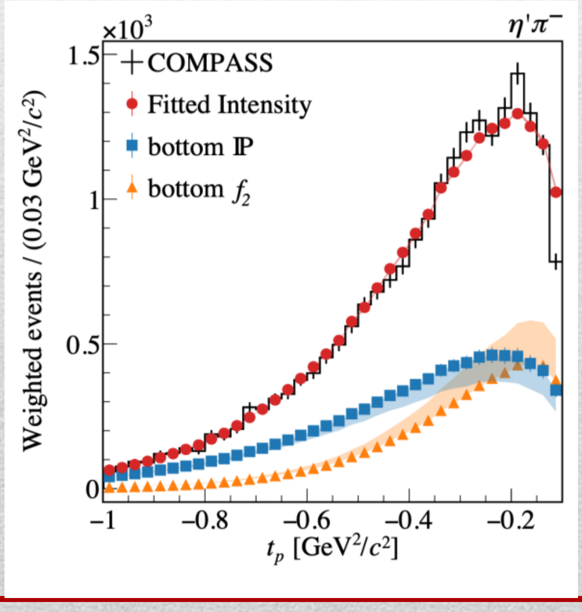

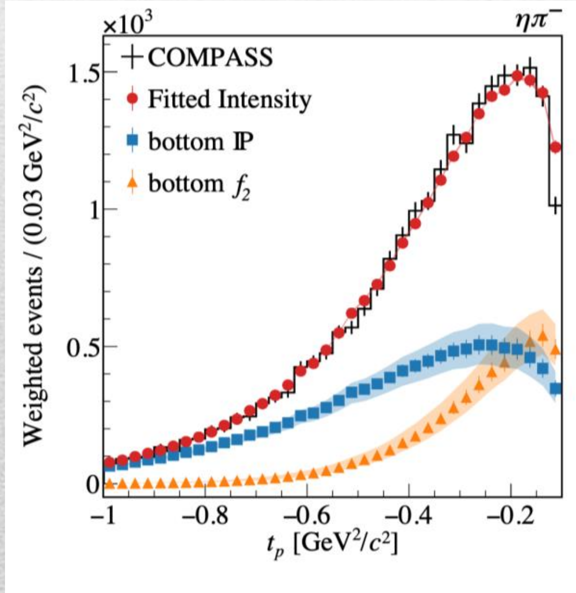

Conclusions

Bottom-up approaches are important!

- They allow us to get the most out of high statistics data!
- AI gives new opportunities for model-independent analyses
- JPAC and ExoHad will continue providing tools and results to understand the exciting spectrum of QCD

Thank you!

BACKUP

Options on the market

Quark-level calculations:

- Quark models, DSE, pNRQCD, Hybrids, ...
- Spectrum generally calculated as bound states of some potential
- Decay rates as «overlap integrals» between two static configurations

Comprehensive picture ✓ Little scattering dynamics ✘

Hadron level calculations:

- Microscopic models inspired to EFT + Unitarization
- Compact states vs. molecules, triangles...
- States as poles of scattering amplitudes
- Couplings as residues at the poles

Scattering dynamics ✓ More case-by-case ✓✘

Potential problems

We can't afford being misguided by simplistic resonance extraction!
(life is already hard enough without red herrings)

Amplitude analysis requires collaboration
of theorists and experimentalists

However, we don't have a universal recipe to do things right
We have to proceed:

- Case-by-case
- Keep in mind the limitations of each approach
- Overstudy (the more approaches the better)
- No overstatement (do-no-harm)

Real(istic) conversations between theorists and experimentalists

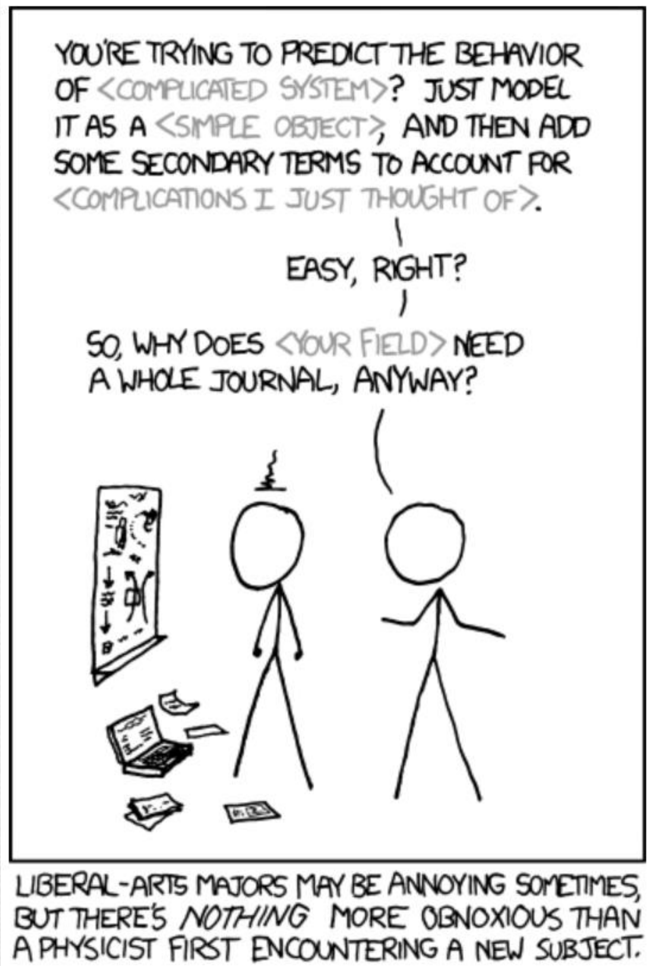

T: How could you not find the XXX quantum numbers?
E: Well, you know, 5D fit, O(100) parameters, local minima, systematics…
T: You are not that good, are you?

T: You shouldn't use Breit Wigners!
E: Gimme some better
T: I have an analytic unitary parametrization, but it works in a given mass window and only knows about energy dependence, you can't add background terms to it…
E: Breit Wigners.

T: Stop using complex couplings!
E: HAHAHAHHAHAHAHAHAHHHAHAHAHA

How theorists think of experiments

All the information about hadrons is collected by the Particle Data Group

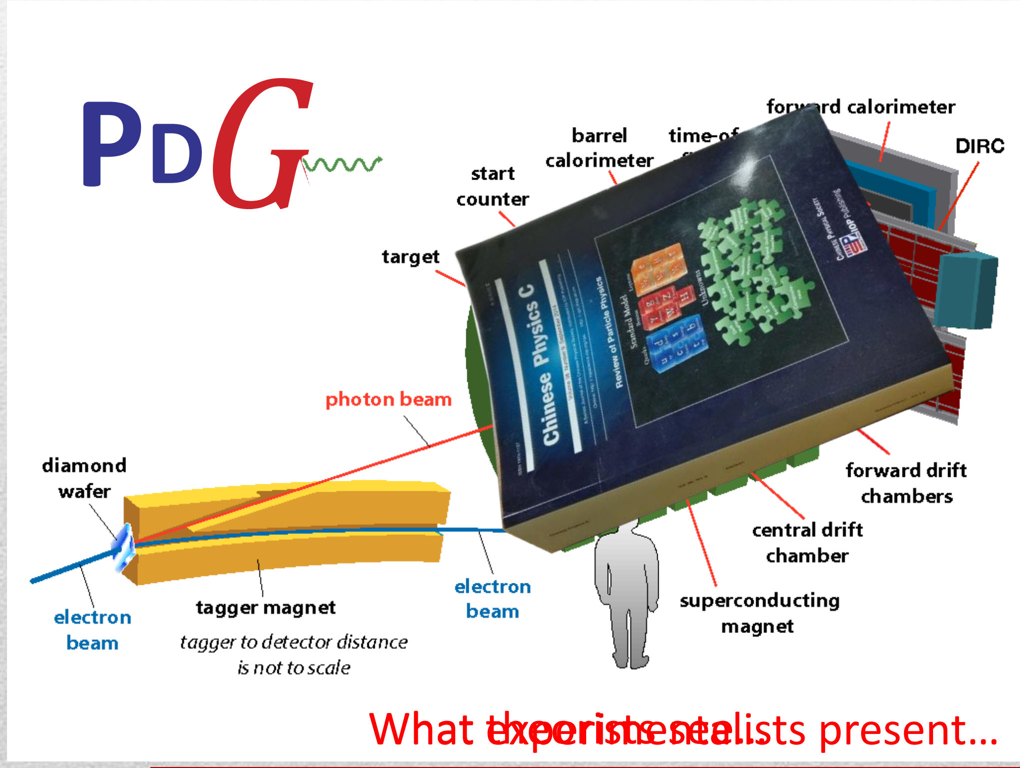

Changing beam and target, you can change the font

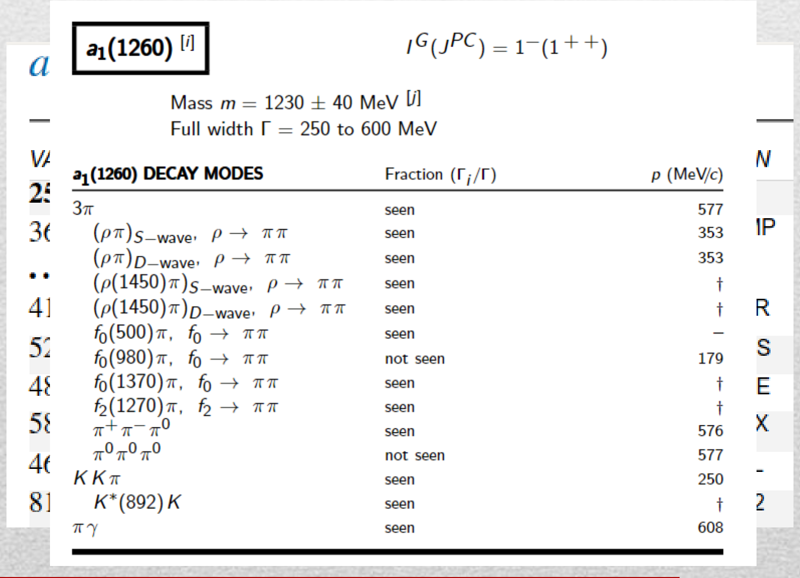

$a_1(1260)$ [i] $I^G(J^{PC}) = 1^-(1^{++})$

Mass $m = 1230 \pm 40$ MeV [j]
Full width $\Gamma = 250$ to 600 MeV

$a_1(1260)$ DECAY MODES	Fraction (Γ_i/Γ)	p (MeV/c)
3π	seen	577
$(\rho\pi)_{S-\text{wave}},\ \rho \to \pi\pi$	seen	353
$(\rho\pi)_{D-\text{wave}},\ \rho \to \pi\pi$	seen	353
$(\rho(1450)\pi)_{S-\text{wave}},\ \rho \to \pi\pi$	seen	†
$(\rho(1450)\pi)_{D-\text{wave}},\ \rho \to \pi\pi$	seen	†
$f_0(500)\pi,\ f_0 \to \pi\pi$	seen	–
$f_0(980)\pi,\ f_0 \to \pi\pi$	not seen	179
$f_0(1370)\pi,\ f_0 \to \pi\pi$	seen	†
$f_2(1270)\pi,\ f_2 \to \pi\pi$	seen	†
$\pi^+\pi^-\pi^0$	seen	576
$\pi^0\pi^0\pi^0$	not seen	577
$KK\pi$	seen	250
$K^*(892)K$	seen	†
$\pi\gamma$	seen	608

Exotics

The quark model is still the simplest tool to organize the spectrum

JPAC, PPNP 127 (2022), 103981

«Exotic hadrons» are Beyond the Standard (quark) Model

Organizing them teaches us some more about quark-gluon interactions

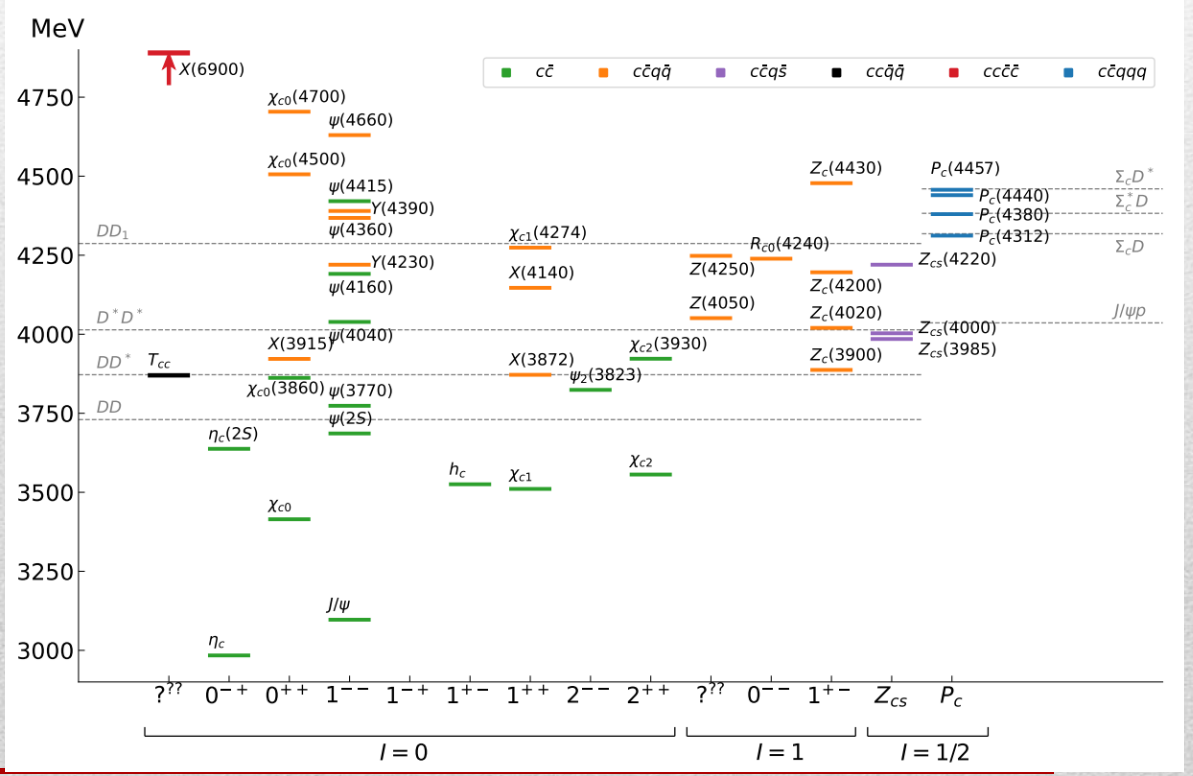

In defense of VMD

The weak point of the whole approach is the use of VMD
While in the light sector it works reasonably, for heavy states is not justified

The X(3872) observed in purely hadronic and photonic modes gives us unique clue to efficacy of VMD

Belle extracted the coupling $X(3872) \to \gamma\gamma^*$,
that can be compared with the VMD predictions
from $X(3872) \to J/\psi\ \rho, \omega$

Q	V	$\mathcal{E}$	$g_{Q\gamma\gamma^*} \times 10^3$
$X(3872)$	γ	γ^*	3.2
	J/ψ	ρ	5.38
		ω	3.54

Other estimate lead to differences of a factor ~ 3

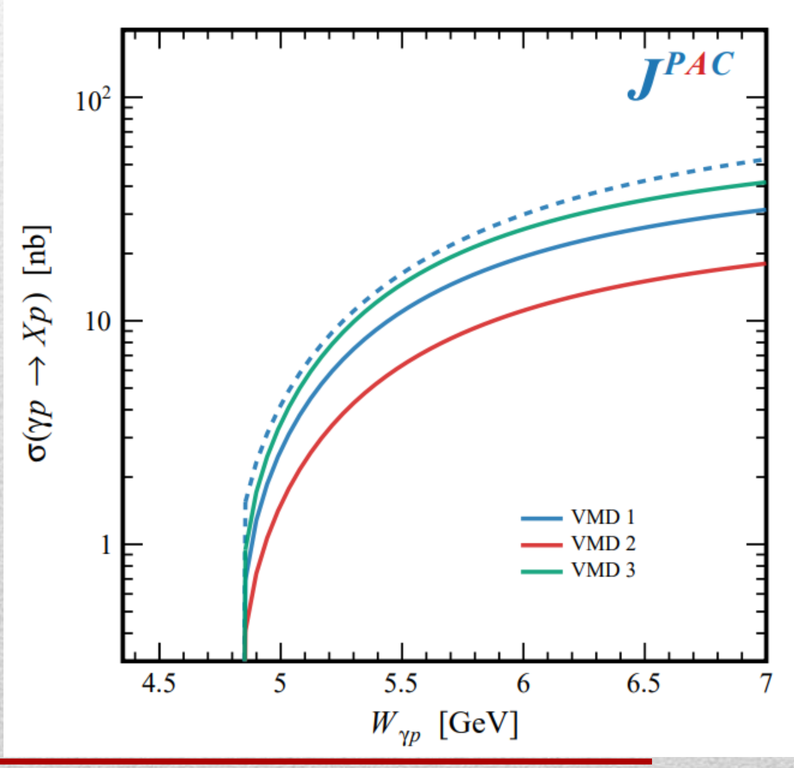

Hadron Spectroscopy

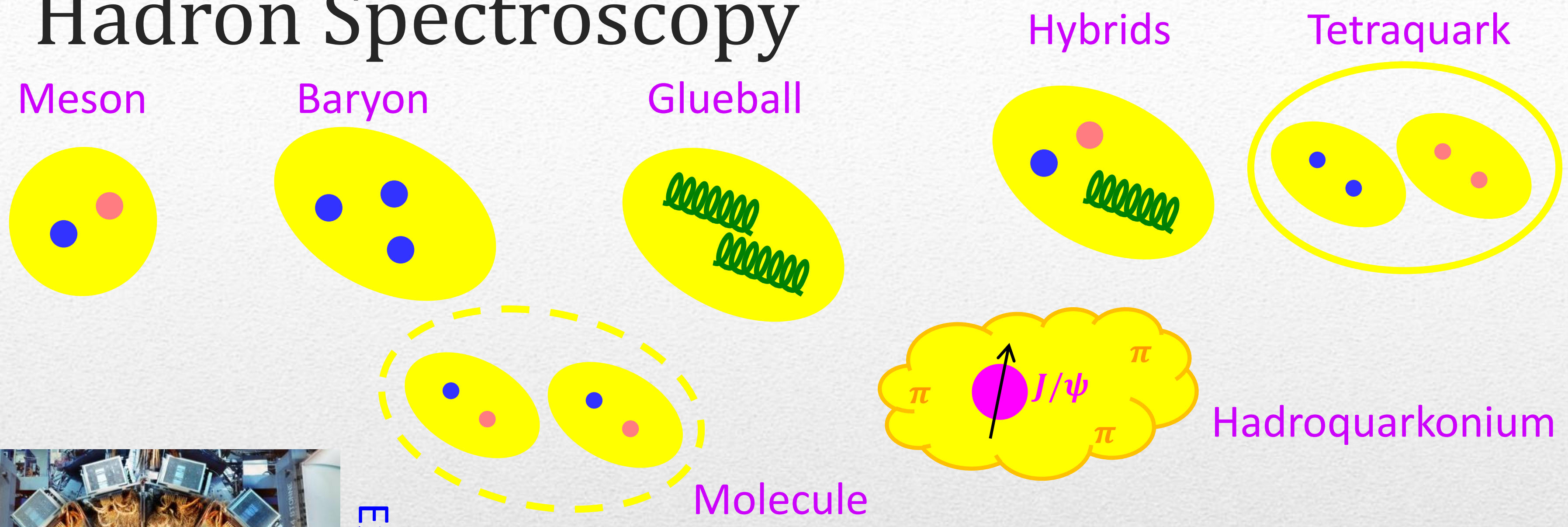

Experiment

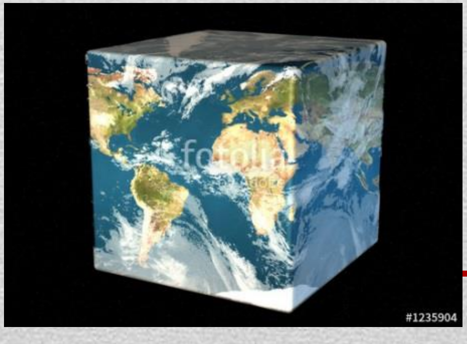

Lattice QCD

Data → Amplitude analysis → QCD

Interpretations on the spectrum leads to understanding fundamental laws of nature

How to identify a glueball

You don't. Since it mixes with light isoscalars, there is no model-independent way of saying which state is (mostly) the glueball. Only suggestions:

- There is one too many wrt QM. Indeed, $f_0(1370), f_0(1500), f_0(1710)$
- A glueball couples to photons only throughout mixing, so radiative widths should be small
- Their production is enhanced in gluon-rich processes, as J/ψ radiative decays
- It couples equally to mesons of all flavors (?)
  However, an argument based on chiral symmetry claims the coupling proportional to quark mass

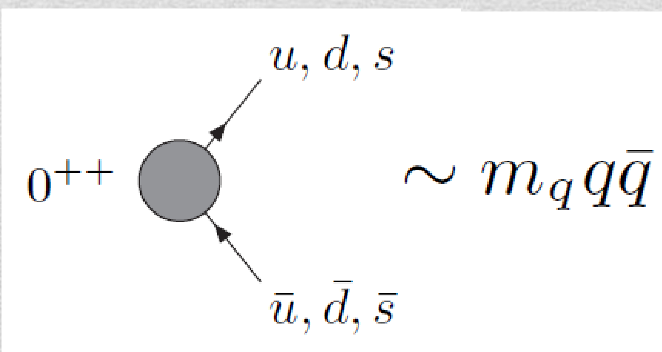

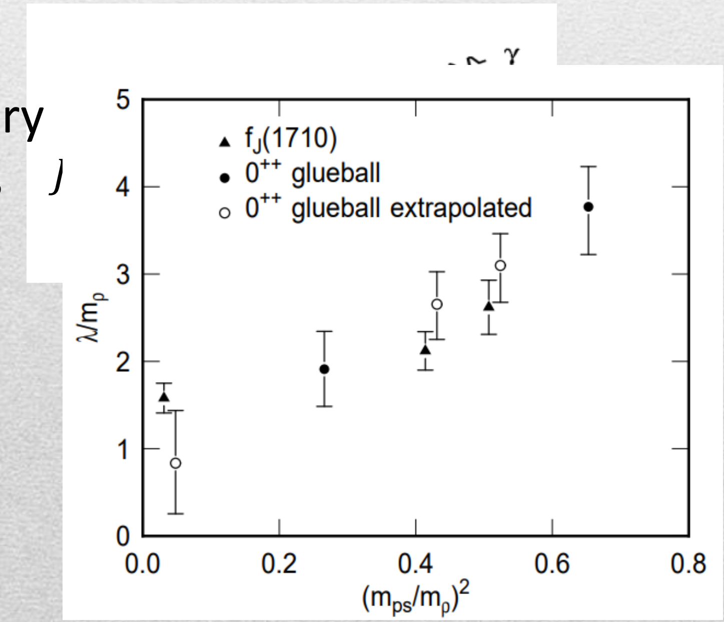

Options on the market

Quark-level calculations:

- Quark models, pNRQCD, Hybrids, ...
- Spectrum generally calculated as bound states of some potential
- Decay rates as «overlap integrals» between two static configurations

Comprehensive picture ✓ Little scattering dynamics ✘

Hadron level calculations:

- Microscopic models inspired to EFT + Unitarization
- Compact states vs. molecules, triangles...
- States as poles of scattering amplitudes
- Couplings as residues at the poles

Scattering dynamics ✓ More case-by-case ✓✘

Hybrid hunting

Constituent gluon (quasiparticle excitation),
$J^{PC} = 1^{+-}$, mass ~ 1.0−1.5 GeV

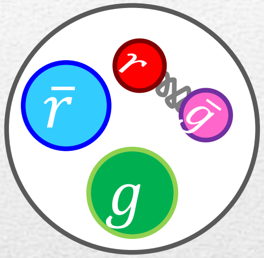

Look for a π_1 state with $\boldsymbol{J^{PC} = 1^{-+}}$

$$\text{decaying into} \begin{cases} \eta\,\pi \text{ and } \eta'\pi \\ \rho\,\pi \to 3\pi \\ b_1\pi \to 5\pi \end{cases}$$

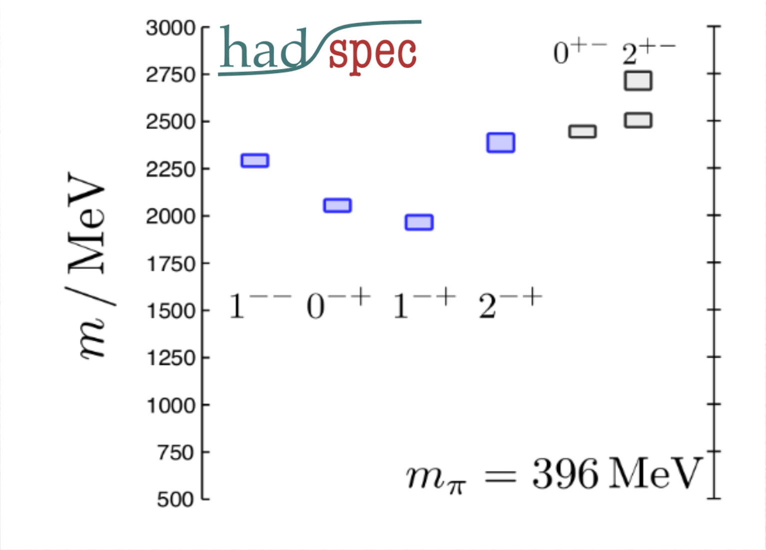

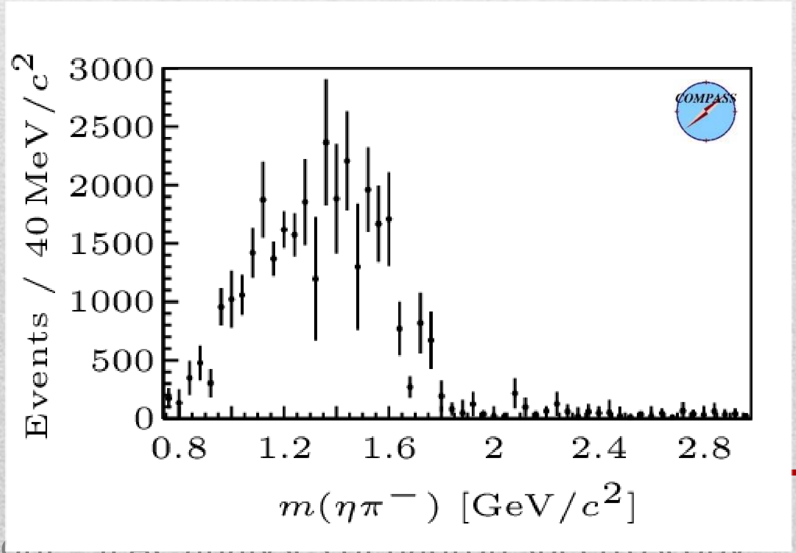

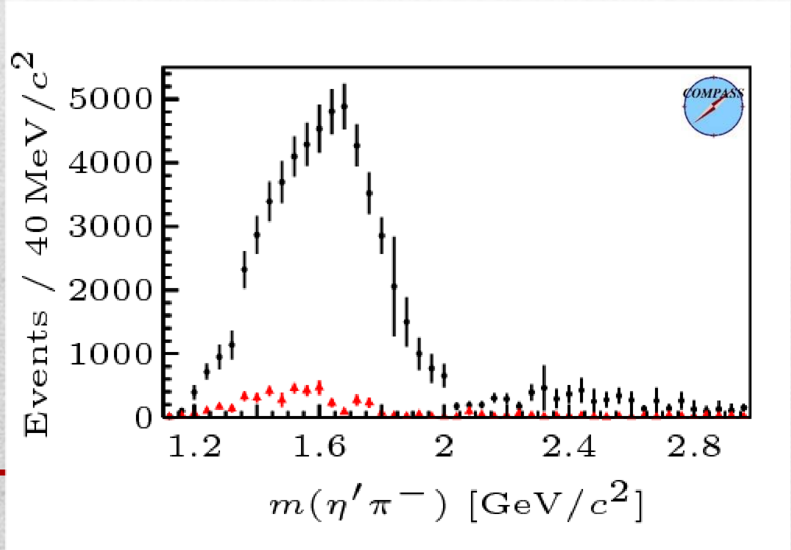

Amplitudes for $\eta^{(\prime)}\pi$

We build the partial wave amplitudes according to the N/D method

Jackura, Mikhasenko, AP *et al.* (JPAC & COMPASS), PLB

Rodas, AP *et al.* PRL

$$a(s) = \frac{n(s)}{D(s)}$$

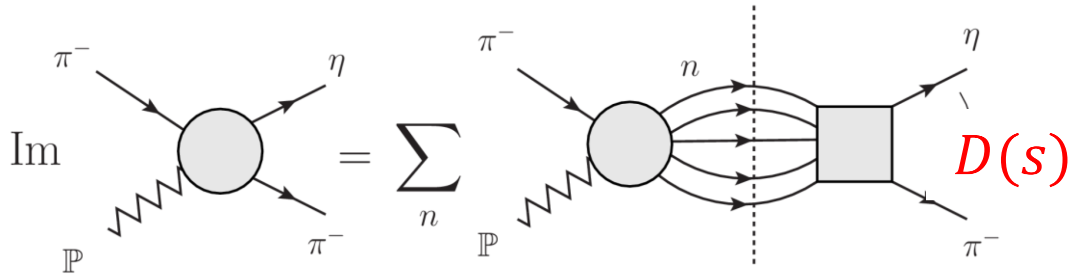

The $D(s)$ contains all the Final State Interactions constrained by unitarity → universal

Amplitudes for $\eta^{(\prime)}\pi$

We build the partial wave amplitudes according to the N/D method

Jackura, Mikhasenko, AP *et al.* (JPAC & COMPASS), PLB

Rodas, AP *et al.* PRL

$$a(s) = \frac{n(s)}{D(s)}$$

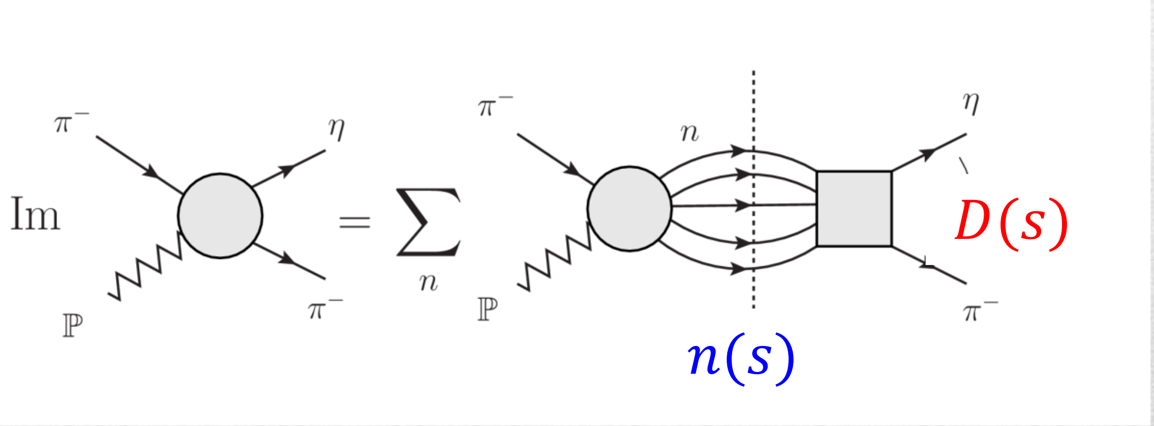

The $n(s)$ → background physics, process-dependent, smooth

Fit to $\eta^{(\prime)}\pi$

(data)

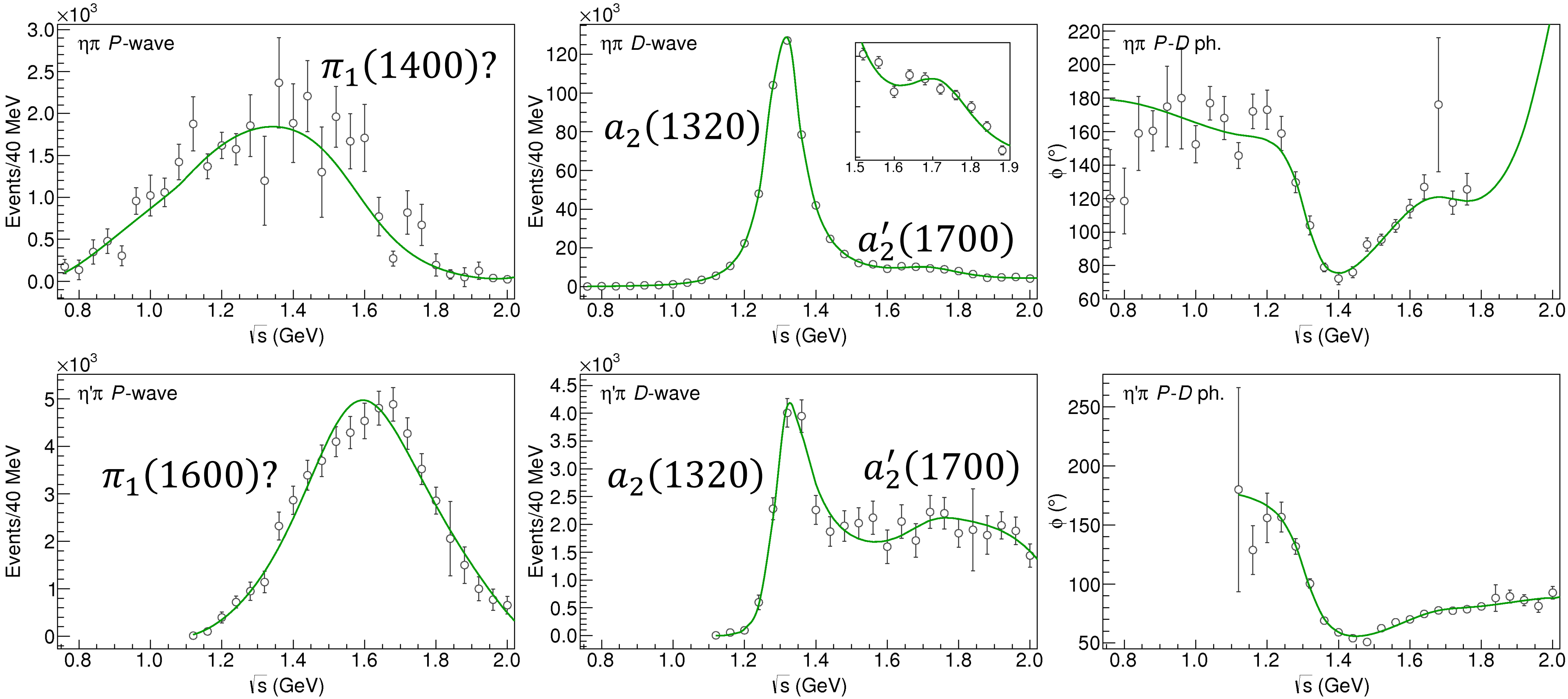

$J^{PC} = 1^{-+}$ $\qquad$ $J^{PC} = 2^{++}$

Pole hunting

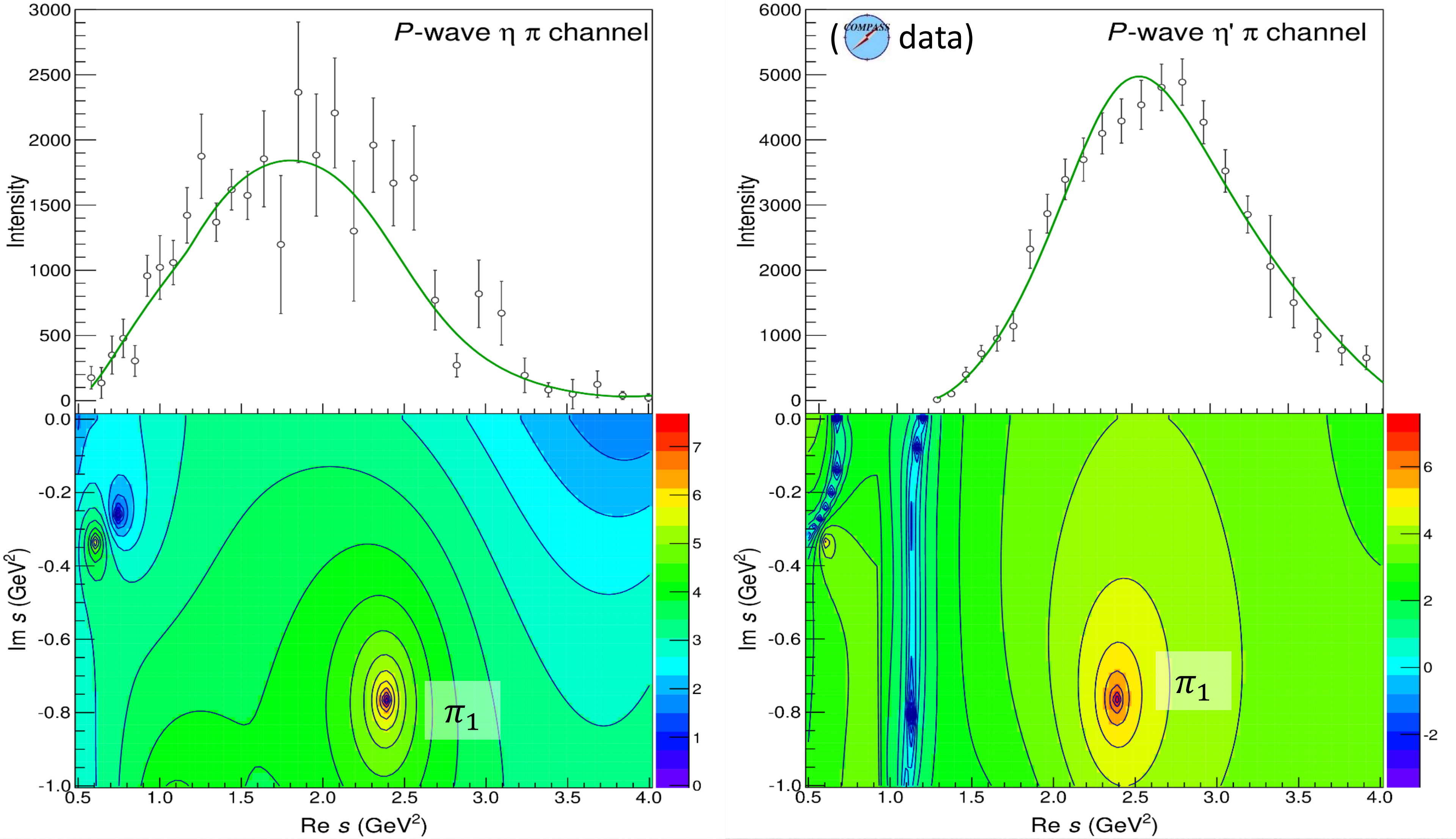

Final results

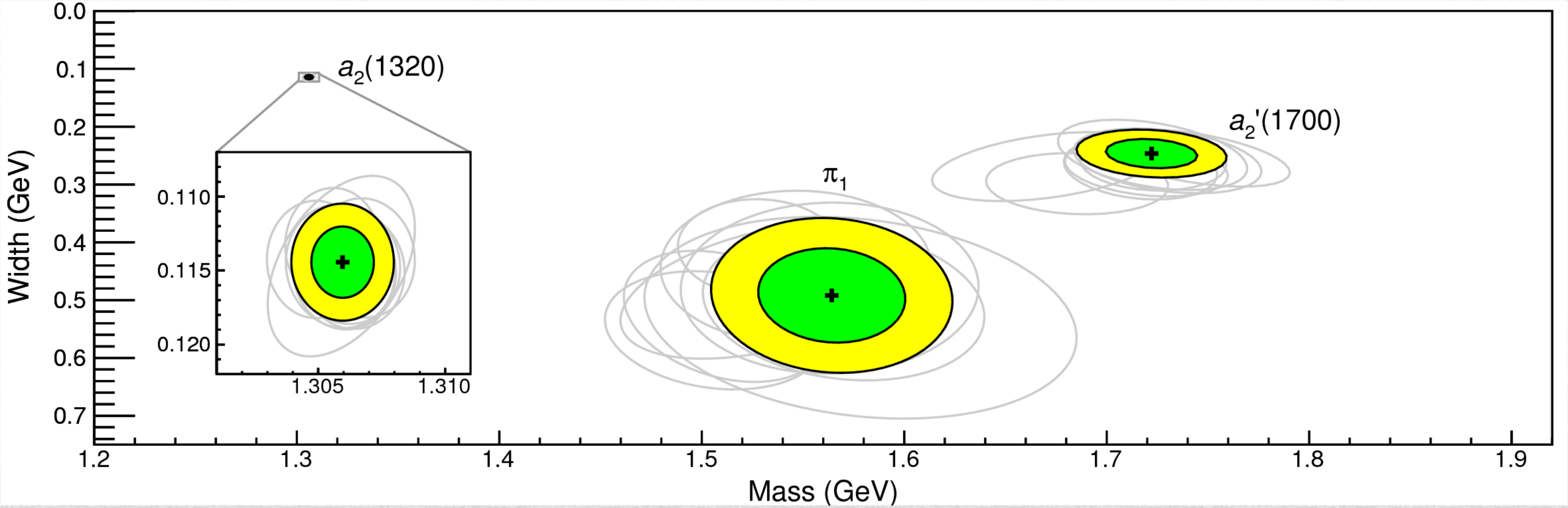

Poles	Mass (MeV)	Width (MeV)
$a_2(1320)$	$1306.0 \pm 0.8 \pm 1.3$	$114.4 \pm 1.6 \pm 0.0$
$a_2'(1700)$	$1722 \pm 15 \pm 67$	$247 \pm 17 \pm 63$
π_1	$1564 \pm 24 \pm 86$	$492 \pm 54 \pm 102$

Agreement with Lattice is restored

That's the most rigorous extraction of an exotic meson available so far!

Glueballs

The clearest sign of confinement in pure Yang-Mills

The worst state to search in real life

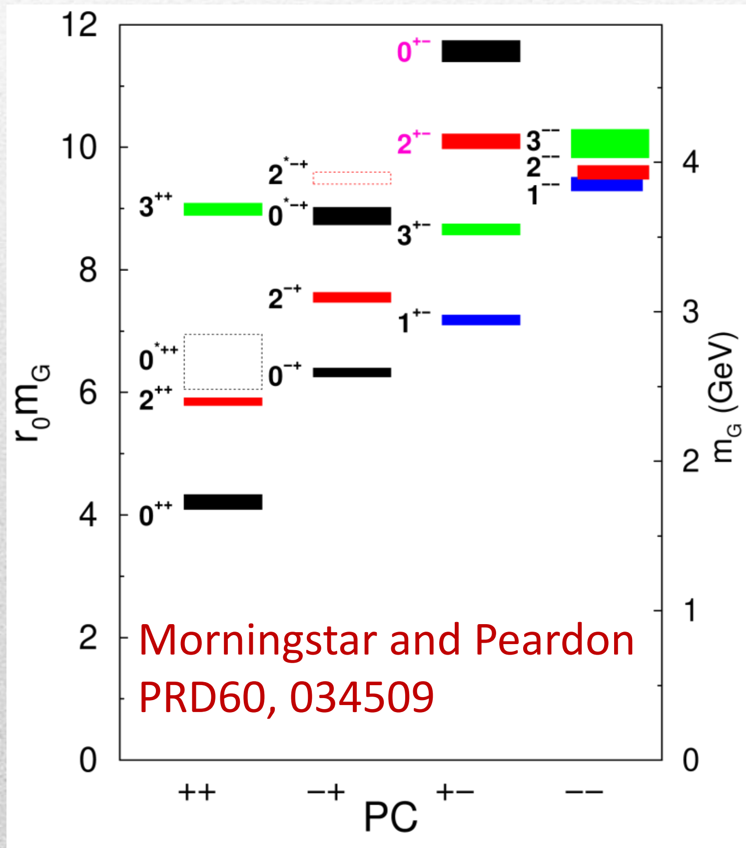

J^{PC}	Mass MeV			
	Unquenched	Quenched		
	This work	M&P	Ky	Meyer
0^{-+}		2590(40)(130)	2560(35)(120)	2250(60)(100)
2^{-+}	3460(320)	3100(30)(150)	3040(40)(150)	2780(50)(130)
0^{-+}	4490(590)	3640(60)(180)		3370(150)(150)
2^{-+}				3480(140)(160)
5^{-+}				3942(160)(180)
0^{--} (exotic)	5166(1000)			
1^{--}		3850(50)(190)	3830(40)(190)	3240(330)(150)
2^{--}	4590(740)	3930(40)(190)	4010(45)(200)	3660(130)(170)
2^{--}				3.740(200)(170)
3^{--}		4130(90)(200)	4200(45)(200)	4330(260)(200)
1^{+-}	3270(340)	2940(30)(140)	2980(30)(140)	2670(65)(120)
3^{+-}	3850(350)	3550(40)(170)	3600(40)(170)	3270(90)(150)
3^{+-}				3630(140)(160)
2^{+-} (exotic)		4140(50)(200)	4230(50)(200)	
0^{+-} (exotic)	5450(830)	4740(70)(230)	4780(60)(230)	
5^{+-}				4110(170)(190)
0^{++}	1795(60)	1730(50)(80)	1710(50)(80)	1475(30)(65)
2^{++}	2620(50)	2400(25)(120)	2390(30)(120)	2150(30)(100)
0^{++}	3760(240)	2670(180)(130)		2755(30)(120)
3^{++}		3690(40)(180)	3670(50)(180)	3385(90)(150)
0^{++}				3370(100)(150)
0^{++}				3990(210)(180)
2^{++}				2880(100)(130)
4^{++}				3640(90)(160)
6^{++}				4360(260)(200)

Gregory *et al.*
JHEP1210, 170

$J/\psi \to \gamma\, \pi^0\pi^0$ and $\to \gamma\, K_S^0 K_S^0$

We consider the S and D wave by BESIII to use the information about their relative phase.

The D-wave is populated by two almost elastic resonances: the $f_2(1270)$ and $f_2'(1525)$